

Competition between epithelial tissue elasticity and surface tension in cancer morphogenesis

Antonino Favata¹ Roberto Paroni² Filippo Recrosi³
Giuseppe Tomassetti⁴

July 27, 2021

¹ Department of Structural and Geotechnical Engineering
Sapienza University of Rome, Rome, Italy
antonino.favata@uniroma1.it

² Dipartimento di Ingegneria Civile e Industriale
Università di Pisa, Pisa, Italy
roberto.paroni@unipi.it

³ Department of Structural and Geotechnical Engineering
Sapienza University of Rome, Rome, Italy
filippo.recrosi@uniroma1.it

⁴ Department of Engineering
Roma Tre University
giuseppe.tomassetti@uniroma3.it

Abstract

We derive a continuum mechanical model to capture the morphological changes occurring at the pretumoral stage of epithelial tissues. The proposed model aims to investigate the competition between the bulk elasticity of the epithelium and the surface tensions of the apical and basal sides. According to this model, when the apico-basal tension imbalance reaches a critical value, a subcritical

bifurcation is triggered and the epithelium attains its physiological folded shape. Based on data available in the literature, our model predicts that pretumoral cells are softer than healthy cells.

Keywords: Epithelium, subcritical bifurcation, surface energy, cancer morphogenesis, rod theories, cell elasticity

Contents

1	Introduction	3
1.1	Physiology of epithelial tissues	3
1.2	Brief survey of available mechanical models	4
1.3	The proposed model and its implications	5
1.4	Organization of the manuscript	6
2	Modeling	6
2.1	Geometry and kinematics	6
2.2	Energetics	9
2.3	Incompressibility	12
2.4	Non-dimensionalization and approximation	13
2.5	Euler-Lagrange equations	14
2.6	The uniformly straight configuration	16
2.7	The boundary value problem	17
3	Critical apico-basal imbalance: loss of positivity of the elasticity tensor	19
4	Bifurcation analysis	25
4.1	Apico-basal tension imbalance yields subcritical bifurcation	29

<i>Epithelial tissue elasticity and surface tension</i>	3
5 Kras oncogene activation makes epithelial cells softer	33
A Properties of the reduced function $f(\eta, \beta)$	38
B Evaluation of $\tilde{\mathbf{u}}_{\eta\eta}$	40

1 Introduction

1.1 Physiology of epithelial tissues

Epithelial tissues are one of the most widespread type of tissue in living things. Epithelia differ in shape and function. They appear in mono or multi-layers of cells covering and protecting the inner parts of tissues and organs. These layers are in the shape of flat sheets in the case of skin, or in the shape of corrugated and folded membranes in stomach and intestine, where they give rise to villi and crypts. These corrugations increase the exchanging area, favoring the secretion of enzymes and absorption of nutrients. During embryogenesis epithelial tissues differentiate from all the three embryonic cell layers, undergoing extensive and precise morphological changes, which result in complex folding patterns.

Epithelial morphogenesis is characterized by a highly complex chemo-mechanical phenomenology which is not comprehensively understood yet, and whose review is out of topic of the present paper. Despite this complexity, the purely mechanical aspects of these processes are key in determining tissural architecture. In particular, it is known that epithelial folding can be the manifestation of a mechanical instability triggered by the contractile action of a meshwork of cross-linked actin filaments acting in the proximity of the apical and basal membranes of the cells (see the sketch in Fig. 2 from Section 2.2 of the present paper).

Epithelia are a common site of tumor onset: Carcinomas, arising from the

epithelium, represent more than 80% of the cancer-related deaths in the Western world [1]. In particular, Pancreatic Ductal Adenocarcinoma (PDAC) is the most lethal of the common cancers, without effective therapeutic option except surgery [2].

1.2 Brief survey of available mechanical models

Perhaps the earliest attempt to understand the mechanical basis of epithelial folding dates back to the work of W.H. Lewis [3], who came up with a two-dimensional physical model consisting of a linear framework of pinned bars, representing an epithelium sheet, with elastic cables stretched on the top and bottom side, which would mimic the apical and the basal tensions. More recently, several mechanical models have been devised: from the 2D and 3D vertex models [4, 5, 6, 7, 8, 9], to continuum models [10, 11], which picture an epithelial layer as a planar rod or as a shell. Among of the latter, some recent works investigate the epithelial tissue morphogenesis as triggered by buckling instability [15, 16, 17, 18, 19, 20, 21, 22] or by differential intraepithelial tensions [23, 24, 25, 26]. In [24, 27, 28] apico-basal differential tension is shown to be enough to produce folded configurations in longitudinal epithelial sheets. In [27] a continuum model, derived from area- and perimeter-elasticity (APE) models [29], is proposed for the healthy epithelium.

Concerning the connection with tumor morphogenesis, as reviewed in [30], the available models address multiple mechanical factors as responsible for the disruption of normal tissue architecture besides the abnormal acto-myosin concentration gradient from basal to apical region [31], which is the mechanical effect that we address in the present paper; in particular, other factors include cancer cells proliferation [11], lateral cell adhesion [23], elasticity of the basement membrane [27].

1.3 The proposed model and its implications

We model an epithelial monolayer as a two dimensional thin body equipped with a bulk and a surface energy at the apical and basal sides. These energetic terms are in competition: the former favors the undeformed configuration; the latter induces bending when the apical and basal energies are imbalanced. By dimension reduction, based on a kinematic Ansatz allowing for thickness extension, we arrive at a one-dimensional model of a nonlinear elastic rod whose equilibria are governed by the competition of the aforementioned energetic contributions.

In our model two dimensionless key parameters are introduced, γ and σ : the former is a measure of the relative importance of surface energy compared to bulk energy; the latter is a measure of the imbalance between apical and basal tensions.

As γ grows, surface energy becomes more important: the apical and basal sides shorten and, in turn, the thickness increases. A growth of σ favors curved configurations.

We formulate a nonlinear equilibrium problem that admits in principle a manifold of solutions. The rectilinear configuration is a solution of this problem for every choice of γ and σ . For γ small, bulk elasticity prevails over surface tension and there is no other solution except the rectilinear one; for γ large enough, there exists a critical value σ_c of the parameter σ where bifurcation from the rectilinear configuration occurs.

A careful analysis, performed through the Lyapunov-Schmidt decomposition, reveals that the bifurcation is subcritical. This is confirmed by our numerical calculations.

Our model predicts a distinctive mechanical behavior of pre-cancerous cells. Based on data available in [31], we estimate the pretumoral tissue softening for pancreatic Neoplasia. This result is in accordance with elastographic measures

in [2], and confirms that transformed cells are softer than healthy cells.

1.4 Organization of the manuscript

In Section 2 we derive our model by prescribing the geometry and the underlying kinematical hypotheses. We specify the form of the bulk and surface energy, and we introduce an incompressibility constraint. We identify the relevant dimensionless parameters, we derive the equilibrium equations, and we formulate a boundary-value problem.

In Section 3 we study the loss of positivity of the elasticity tensor and we determine the critical value of the apico-basal tension imbalance, along with the bifurcation mode.

In Section 4 we perform a detailed bifurcation analysis by means of the Lyapunov-Schmidt decomposition, and we identify the type of bifurcation. We accompany our analysis with a numerical calculation.

In Section 5 we discuss the implication of our model concerning the softening which accompanies incipient tumorigenesis.

2 Modeling

2.1 Geometry and kinematics

In line with recent work addressing folding patterns through continuum models [24, 32], we restrict our attention to planar deformations. In accordance with this point of view, we identify a single layer of epithelial cells with a thin strip Ω of length ℓ and finite thickness h , and we choose an Ansatz on the class of possible deformations which will lead us to a one-dimensional model of a rod deforming on a plane.

One of the features of our approach is that our Ansatz involves a scalar pa-

parameter μ (see (4) below) which describes transverse extension/contraction of the epithelial sheet, as observed in experiments (see, *e.g.*, [31]). We take into account the overall incompressibility of the epithelial sheet by enforcing volume conservation *on average* along the thickness (see (15) and (17) below). The resulting model predicts that the ability of the epithelium to undergo transversal stretching and contraction is a key ingredient for the bifurcations that mark the transition from flat to folded configurations. This idea is not new in mechanics: bending instabilities of rods accompanied by non-uniform striction and/or dilation of the transversal fibers manifest themselves with the *Brazier effect* [33, 34, 35, 36].

To describe our Ansatz, we introduce a coordinate system (x_1, x_2) , and we let $\{\mathbf{e}_1, \mathbf{e}_2\}$ be the associated orthonormal basis (see Fig.1). We assume that

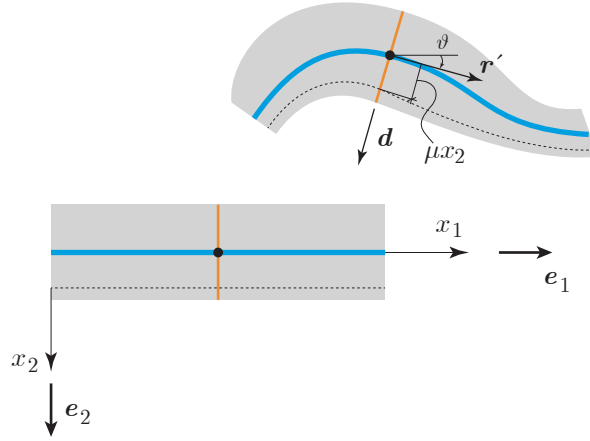


Figure 1: The strip in the reference and in the deformed configuration. As in standard rod theories, the transversal fiber (orange segment) remains straight and orthogonal to the mid axis (blue curve), but may undergo stretching.

the deformation has the form:

$$\mathbf{f}(x_1, x_2) = \mathbf{r}(x_1) + x_2 \mathbf{d}(x_1). \quad (1)$$

The vectors $\mathbf{r}(x_1)$ and $\mathbf{d}(x_1)$ represent, respectively, the position of the midline of the epithelium and the orientation of the typical transversal fiber. We allow the midline and the transverse direction to change length, thus the vectors $\mathbf{r}'(x_1)$ and $\mathbf{d}(x_1)$ are not necessarily of unit length, but we assume that the transverse sections remain orthogonal to the midline curve:

$$\mathbf{r}' \cdot \mathbf{d} = 0.$$

Accordingly, the deformation gradient is

$$\mathbf{F} = \nabla \mathbf{f} = (\mathbf{r}' + x_2 \mathbf{d}') \otimes \mathbf{e}_1 + \mathbf{d} \otimes \mathbf{e}_2. \quad (2)$$

We denote by $\vartheta(x_1)$ the rotation of the director $\mathbf{d}(x_1)$ with respect to the reference configuration. Then the unit vectors

$$\mathbf{a}_1 := \frac{\mathbf{r}'}{|\mathbf{r}'|} = \cos \vartheta \mathbf{e}_1 + \sin \vartheta \mathbf{e}_2, \quad \text{and} \quad \mathbf{a}_2 := -\sin \vartheta \mathbf{e}_1 + \cos \vartheta \mathbf{e}_2. \quad (3)$$

represent, respectively, the tangent and the normal to the axis in the deformed configuration; a prime denotes differentiation with respect to the coordinate x_1 . Thus, we can write

$$\mathbf{r}' = \lambda \mathbf{a}_1, \quad \mathbf{d} = \mu \mathbf{a}_2, \quad (4)$$

where λ and μ are, respectively, the *axial* and *transverse stretch*.

From (3), $\mathbf{a}'_2 = -\vartheta' \mathbf{a}_1$, hence $\mathbf{d}' = \mu' \mathbf{a}_2 - \mu \vartheta' \mathbf{a}_1$ and the deformation gradient given in (2) can be rewritten as

$$\mathbf{F} = (\lambda - x_2 \mu \vartheta') \mathbf{a}_1 \otimes \mathbf{e}_1 + x_2 \mu' \mathbf{a}_2 \otimes \mathbf{e}_1 + \mu \mathbf{a}_2 \otimes \mathbf{e}_2. \quad (5)$$

We next introduce the local rotation:

$$\mathbf{R} := \mathbf{a}_1 \otimes \mathbf{e}_1 + \mathbf{a}_2 \otimes \mathbf{e}_2 \quad (6)$$

which maps the reference basis $\{\mathbf{e}_1, \mathbf{e}_2\}$ onto the current basis $\{\mathbf{a}_1, \mathbf{a}_2\}$. Since we have in mind to deduce a beam-like model, we choose as deformation measure

$$\mathbf{D} := \mathbf{R}^\top \mathbf{F} = (\lambda - x_2 \mu \vartheta') \mathbf{e}_1 \otimes \mathbf{e}_1 + x_2 \mu' \mathbf{e}_2 \otimes \mathbf{e}_1 + \mu \mathbf{e}_2 \otimes \mathbf{e}_2. \quad (7)$$

The strain measure \mathbf{D} makes free the deformation gradient \mathbf{F} from the rigid rotation of the axis. In the above equation, the last term on the right-hand side is the *transverse stretch*. The first term is the sum of an *average axial stretch* $\lambda \mathbf{e}_1 \otimes \mathbf{e}_1$, plus a linear term proportional to the *curvature* ϑ' of the axis, weighted by $x_2 \mu$, the latter representing the distance from the axis in the *deformed configuration* (see Fig. 1). The second term describes a *non-uniform shear* deformation associated to a possible non-uniformity of the transverse stretch.

2.2 Energetics

In our model we incorporate two different energetic contributions: a *bulk energy* and a *surface energy*. The former accounts for mechanical response of the cytoplasm, here assumed to be elastic; the latter takes into account the *contractile tension* due to the thin meshwork of actin filaments laying beneath the cell membrane, depicted in the cartoons (b) and (c) in Fig. 2 below. In line with existing discrete models which consider an epithelial monolayer as a polygonal tessellation where each side of a polygon carries an energy proportional to its length, we assume that the surface energy be proportional to the tangential stretch at the boundary. This point of view has been already applied in [24]

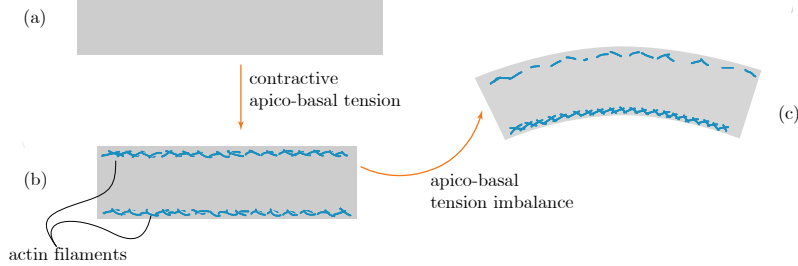


Figure 2: In the absence of surface tension and external load the strip is in equilibrium in the reference configuration (a). The balanced contractile tension of the actin filaments on the upper and lower side the strip induces lateral contraction, and in turn transverse stretching due to incompressibility (b). Imbalance between contractile tension on the upper and lower sides of the strip results in the bent shape (c).

and [32] to derive continuum models for epithelial monolayers.

The consequences of including surface tension on the boundary of an elastic body have already been explored [37, 38, 25], and it is known that it can generate relevant mechanical effects on soft elastic bodies at small scales. In the present setting, however, we allow for an imbalance between the internal forces localized on the apical (top) and basal (bottom) sides of the strip which produces bending, as schematically depicted in Fig. 2-c.

We assume that the material is homogeneous and isotropic, and that it is in its natural state in the reference configuration. As a result, approximating the bulk energy with its Taylor expansion up to second order, we obtain:

$$W_b(\mathbf{F}) = W_b(\mathbf{D}) \simeq \frac{1}{2} D^2 W_b(\mathbf{I}) [\text{sym}(\mathbf{D} - \mathbf{I}), \text{sym}(\mathbf{D} - \mathbf{I})]; \quad (8)$$

the terms $W_b(\mathbf{I})$ and $DW_b(\mathbf{I})$ do not appear since the reference is assumed to be natural, while the dependence on the symmetric part of $\mathbf{D} - \mathbf{I}$ follows from the frame indifference of the energy density W_b .

The assumption that the bulk energy is isotropic entails that there exist

constants α_1 and α_2 such that

$$\frac{1}{2}D^2W_b(\mathbf{I})[\text{sym}(\mathbf{D}-\mathbf{I}), \text{sym}(\mathbf{D}-\mathbf{I})] = \alpha_1 |\text{sym}(\mathbf{D}-\mathbf{I})|^2 + \alpha_2 (\text{tr}(\mathbf{D}-\mathbf{I}))^2. \quad (9)$$

Hereafter, we assume the two material constants α_1 and α_2 to be strictly positive. The bulk strain energy per unit length along the direction x_1 is

$$\int_{-h/2}^{+h/2} W_b(\mathbf{D}) dx_2 = w_b, \quad (10)$$

where

$$w_b(\lambda, \mu, \vartheta') = h \left[\alpha_1 (\lambda^2 + \mu^2) + \alpha_2 (\lambda + \mu)^2 - (\alpha_1 + 4\alpha_2)(\lambda + \mu) \right] + \frac{h^3}{12} \left[\alpha_1 \left(\mu^2 \vartheta'^2 + \frac{\mu'^2}{2} \right) + \alpha_2 \mu^2 \vartheta'^2 \right]. \quad (11)$$

The first term in the above equation, proportional to the thickness, is a *stretching energy*; the second term, which scales as the third power of the thickness, is a *bending energy*.

In order to introduce the surface energy, let us consider an infinitesimal fiber parallel to the \mathbf{e}_1 direction in the reference configuration. The deformation transforms this fiber into, see (5),

$$\mathbf{F}\mathbf{e}_1 = (\lambda - x_2\mu\vartheta') \mathbf{a}_1 + x_2\mu' \mathbf{a}_2. \quad (12)$$

Accordingly, the length of the generic fiber in the deformed configuration is

$$|\mathbf{F}\mathbf{e}_1| = \sqrt{(\lambda - x_2\mu\vartheta')^2 + (x_2\mu')^2}. \quad (13)$$

The surface energy is introduced as the cost paid to stretch the apical and

basal fibers, *i.e.*, $x_2 = \mp h/2$, respectively. On denoting by σ_a and σ_b the apical and basal tensions, (13) allows to define the surface energy per unit length as follows:

$$w_s(\lambda, \mu, \vartheta') = \sigma_a \sqrt{\left(\lambda + \frac{h}{2}\mu\vartheta'\right)^2 + \frac{h^2\mu'^2}{4}} + \sigma_b \sqrt{\left(\lambda - \frac{h}{2}\mu\vartheta'\right)^2 + \frac{h^2\mu'^2}{4}}. \quad (14)$$

We assume σ_a and σ_b to be non-negative.

2.3 Incompressibility

The cells in the epithelial monolayer, being filled with fluid, should be treated as incompressible [24, 32]. Since each cell spans the entire thickness of the body, we find it appropriate to impose incompressibility on average over the thickness:

$$\frac{1}{h} \int_{-h/2}^{+h/2} \det \mathbf{F} dx_2 = 1, \quad (15)$$

where

$$\det \mathbf{F} = \mathbf{F}\mathbf{e}_1 \times \mathbf{F}\mathbf{e}_2 \cdot \mathbf{e}_3 = (\mathbf{r}' + x_2\mathbf{d}') \times \mathbf{d} \cdot \mathbf{e}_3. \quad (16)$$

By combining (16) and (15) we obtain that the product of the longitudinal and transversal stretching is equal to one:

$$\lambda\mu = 1. \quad (17)$$

From this identity we find $\lambda = 1/\mu$ and hence, by dropping additive constants, we can rewrite the energy densities in terms of μ and ϑ , only:

$$w_b(\mu, \mu', \vartheta') = h \left((\alpha_1 + \alpha_2) \left(\frac{1}{\mu^2} + \mu^2 \right) - (\alpha_1 + 4\alpha_2) \left(\frac{1}{\mu} + \mu \right) \right) + \frac{h^3}{12} \left[(\alpha_1 + \alpha_2) \mu^2 \vartheta'^2 + \alpha_1 \frac{\mu'^2}{2} \right] \quad (18)$$

and

$$w_s(\mu, \mu', \vartheta') = \sigma_a \sqrt{\left(\frac{1}{\mu} + \frac{h}{2}\mu\vartheta'\right)^2 + \frac{h^2\mu'^2}{4}} + \sigma_b \sqrt{\left(\frac{1}{\mu} - \frac{h}{2}\mu\vartheta'\right)^2 + \frac{h^2\mu'^2}{4}}. \quad (19)$$

The total energy is simply given by

$$\mathcal{E} = \int_0^\ell w(\mu, \mu', \vartheta') dx, \quad (20)$$

where $w = w_b + w_s$. Note that we have used, and from here on we use, the symbol x to denote the variable x_1 .

2.4 Non-dimensionalization and approximation

We find it convenient to work with adimensional quantities. For this reason, we introduce the following parameters

$$\varepsilon = \frac{h}{\ell}, \quad \alpha = \frac{\alpha_1}{\alpha_1 + \alpha_2}, \quad \sigma = \frac{1}{2} \frac{\sigma_a - \sigma_b}{\sigma_a + \sigma_b}, \quad \gamma = \frac{\sigma_a + \sigma_b}{\ell(\alpha_1 + \alpha_2)}. \quad (21)$$

The parameters ε, α , and γ are non-negative. We will refer to σ as the *apico-basal imbalance parameter*, which will have a pivotal role in our analysis. Then (20) becomes

$$\mathcal{E} = (\alpha_1 + \alpha_2)\ell^2 \int_0^1 \tilde{w} d\tilde{x}, \quad (22)$$

where we have set

$$\tilde{x} = \frac{x}{\ell}, \quad \tilde{w} = \tilde{w}_b + \gamma\tilde{w}_s, \quad (23)$$

and where we have defined the dimensionless surface and bulk energies as, respectively,

$$\begin{aligned} \tilde{w}_s = & \frac{1}{2} \left(\sqrt{\left(\frac{1}{\tilde{\mu}} + \frac{\varepsilon}{2}\tilde{\mu}\tilde{\vartheta}'\right)^2 + \frac{\varepsilon^2\tilde{\mu}'^2}{4}} + \sqrt{\left(\frac{1}{\tilde{\mu}} - \frac{\varepsilon}{2}\tilde{\mu}\tilde{\vartheta}'\right)^2 + \frac{\varepsilon^2\tilde{\mu}'^2}{4}} \right) \\ & + \frac{\sigma}{2} \left(\sqrt{\left(\frac{1}{\tilde{\mu}} + \frac{\varepsilon}{2}\tilde{\mu}\tilde{\vartheta}'\right)^2 + \frac{\varepsilon^2\tilde{\mu}'^2}{4}} - \sqrt{\left(\frac{1}{\tilde{\mu}} - \frac{\varepsilon}{2}\tilde{\mu}\tilde{\vartheta}'\right)^2 + \frac{\varepsilon^2\tilde{\mu}'^2}{4}} \right) \end{aligned} \quad (24)$$

and

$$\tilde{w}_b = \frac{\mathcal{E}_b}{(\alpha_1 + \alpha_2)\ell} = \varepsilon \left(\frac{1}{\tilde{\mu}^2} + \tilde{\mu}^2 \right) + \frac{\varepsilon^3}{12} \left(\tilde{\mu}^2\tilde{\vartheta}'^2 + \alpha \frac{\tilde{\mu}'^2}{2} \right). \quad (25)$$

Note that $\tilde{w} = \frac{w_b + w_s}{\ell(\alpha_1 + \alpha_2)}$. In what follows we drop tildas.

Since the bulk energy involves powers of ε up to the third order, for consistency, we expand the surface energy up to the same order:

$$w_s \simeq \frac{1}{\mu} + \frac{1}{2}\sigma\varepsilon\mu\vartheta' + \frac{1}{8}\varepsilon^2\mu(\mu')^2 - \frac{1}{16}\sigma\varepsilon^3\mu^3\vartheta'(\mu')^2.$$

The total energy that we consider hereafter is

$$\begin{aligned} w = & \varepsilon \left(\frac{1}{\mu^2} + \mu^2 - (4 - 3\alpha) \left(\frac{1}{\mu} + \mu \right) \right) + \frac{\varepsilon^3}{12} \left(\mu^2(\vartheta')^2 + \alpha \frac{(\mu')^2}{2} \right) \\ & + \gamma \left(\frac{1}{\mu} + \frac{1}{2}\sigma\varepsilon\mu\vartheta' + \frac{1}{8}\varepsilon^2\mu(\mu')^2 - \frac{1}{16}\sigma\varepsilon^3\mu^3\vartheta'(\mu')^2 \right). \end{aligned} \quad (26)$$

2.5 Euler-Lagrange equations

On denoting by $\partial_i w$ the partial derivative of w with respect to the i -th argument, the Euler-Lagrange equations of the variational problem are

$$\begin{cases} \partial_1 w(\mu, \mu', \vartheta') - (\partial_2 w(\mu, \mu', \vartheta'))' = 0, \\ (\partial_3 w(\mu, \mu', \vartheta'))' = 0, \end{cases} \quad (27)$$

while the natural boundary conditions are

$$\begin{cases} \mu = \mu_b & \text{or} & \partial_2 w = 0, \\ \vartheta = \vartheta_b & \text{or} & \partial_3 w = 0, \end{cases} \quad (28)$$

where μ_b and ϑ_b are given.

Before proceeding, we find it worth observing that the system of Euler-Lagrange equations is autonomous; as a result, we can transform it into a first-order system by introducing two integration constants. Although we do not make use of this observation in the present paper, it might prove useful for further work, and therefore we sketch the derivation. The second equation of (27) can be integrated to give:

$$\partial_3 w(\mu, \mu', \vartheta') = M, \quad (29)$$

where M is a constant. Also, noticing that

$$\begin{aligned} (w - \mu' \partial_2 w)' &= \partial_1 w \mu' + \partial_2 w \mu'' + \partial_3 w \vartheta'' - \mu'' \partial_2 w - \mu' (\partial_2 w)' \\ &= (\partial_1 w - (\partial_2 w)') \mu' + \partial_3 w \vartheta'' \\ &= M \vartheta'', \end{aligned} \quad (30)$$

where the last equality has been obtained by using (27) and (29), we deduce that there is a constant C such that

$$w(\mu, \mu', \vartheta') - \mu' \partial_2 w(\mu, \mu', \vartheta') = M \vartheta' + C. \quad (31)$$

Equations (29) and (31) can be used in place of (27).

2.6 The uniformly straight configuration

By a uniformly straight configuration we mean a configuration of the form

$$\mu(x) = \bar{\mu}_0, \quad \vartheta(x) = \bar{\vartheta}_0, \quad (32)$$

with $\bar{\mu}_0$ and $\bar{\vartheta}_0$ constant. Since the Euler-Lagrange equations are invariant under rigid rotations, we may take, without loss of generality, $\bar{\vartheta}_0 = 0$.

We now show that for every value of the parameters $\varepsilon, \alpha, \sigma$, and γ there is a uniformly straight configuration, characterized by a particular value of $\bar{\mu}_0$, that satisfies the Euler-Lagrange equations. Indeed, this is quite simple to check by means of (27). In fact, since $\partial_2 w(\bar{\mu}_0, 0, 0)$ and $\partial_3 w(\bar{\mu}_0, 0, 0)$ are constant, the equations (27) simply reduce to

$$\partial_1 w(\bar{\mu}_0, 0, 0) = 0. \quad (33)$$

This equation can be used to find $\bar{\mu}_0$. By evaluating

$$w(\bar{\mu}_0, 0, 0) = \frac{\varepsilon + \gamma\bar{\mu}_0 + \varepsilon(\bar{\mu}_0^4 - (4 - 3\alpha)(\bar{\mu}_0 + \bar{\mu}_0^3))}{\bar{\mu}_0^2}, \quad (34)$$

we find

$$\partial_1 w(\bar{\mu}_0, 0, 0) = \frac{(\bar{\mu}_0^2 - 1)(2 - \bar{\mu}_0(4 - 3\alpha - 2\bar{\mu}_0))\varepsilon - \gamma\bar{\mu}_0}{\bar{\mu}_0^3}. \quad (35)$$

Equation (33) leads to

$$g(\bar{\mu}_0) := \bar{\mu}_0^4 - \frac{\gamma}{2\varepsilon}\bar{\mu}_0 - \frac{4 - 3\alpha}{2}\bar{\mu}_0(\bar{\mu}_0^2 - 1) - 1 = 0, \quad (36)$$

and it is easily concluded that g has only one positive root (see. Fig. 3), hereafter denoted by μ_0 .

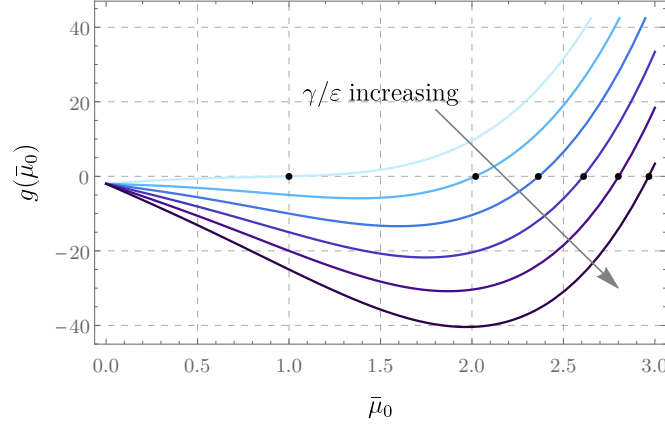


Figure 3: Function $g(\bar{\mu}_0)$ in (36), for fixed $\alpha = 0.2$. The points where $g(\bar{\mu}_0)$ vanishes correspond to the value of μ in the straight configuration. We notice that, when the surface energy has a more and more prevalent role, the thickness of body increases.

Moreover, since $g(1) = -\gamma/(2\varepsilon) \leq 0$, we see that

$$\mu_0 \geq 1 \quad \text{and} \quad \mu_0 = 1 \iff \gamma = 0. \quad (37)$$

Thus, if the surface energy is not “activated” ($\gamma = 0$) there is no stretching of the transversal sections $\mu_0 = 1$ and by the incompressibility constraint, (17), also the axial stretching is absent. This is clearly consistent with the assumption of natural reference configuration. While, if the surface energy is “activated” ($\gamma > 0$), the surface area is penalized and hence the axial stretching decreases. By the incompressibility constraint it follows that the transversal sections are stretched: $\mu_0 > 1$.

2.7 The boundary value problem

We consider the following boundary conditions:

$$\mu(x) = \mu_0, \quad \vartheta(x) = 0 \quad \text{for} \quad x = 0, 1,$$

where μ_0 is the root of (37). From Section 2.6 we know that configurations of the form

$$\mu(x) = \mu_0, \quad \vartheta(x) = \vartheta_0$$

satisfy the equilibrium equations.

As detailed in the Introduction, experimental evidences show that imbalance between apical and basal surface tension may induce a change of shape in cancerous epithelial tissues; thus, we investigate the existence of other (non trivial) solutions as the apico-basal imbalance parameter σ changes. It is convenient to set

$$\xi(x) = \mu(x) - \mu_0(x)$$

and to denote by

$$\mathbf{u} = (\xi, \vartheta)$$

the pair of independent variables. We shall explicitly write the dependence of the energy on σ

$$\mathcal{E}(\mathbf{u}, \sigma) = \int_0^1 w(\mu_0 + \xi, \xi', \vartheta') dx$$

where w is given by (26). The equilibrium equations are

$$0 = d\mathcal{E}(\mathbf{u}, \sigma)[\mathbf{v}] = \left. \frac{d}{ds} \mathcal{E}(\mathbf{u} + s\mathbf{v}, \sigma) \right|_{s=0} \quad \forall \mathbf{v}; \quad (38)$$

every time we write $\forall \mathbf{v}$, we mean for every ξ, ϑ smooth that are null at 0 and 1. This equation, after integration by parts and localization, is equivalent to (27). Since the uniformly straight configuration $\xi = 0$ and $\vartheta = 0$ satisfies the equilibrium condition for every σ , we have that

$$d\mathcal{E}(\mathbf{o}, \sigma)[\mathbf{v}] = 0 \quad \forall \mathbf{v} \text{ and } \forall \sigma \quad (39)$$

where we have set

$$\mathbf{o} = (0, 0).$$

3 Critical apico-basal imbalance: loss of positivity of the elasticity tensor

As reported in the Introduction, in [31] it has been observed, by detecting the intensity of pMLC2 staining on the apical and the basal side of an epithelium, that the difference between the apical and basal surface tension is considerably higher in wild-type cells than in transformed cells. This means that the parameter σ , which measures the surface tension apico-basal imbalance, in transformed cells is small compared to the value assumed by σ in wild-type cells. From this consideration a natural question arises: do the sole change of σ leads to a morphological transition? From Section 2.6 we know that for every value of σ there is a uniformly straight configuration and hence if a morphological transformation occurs we will have more than one solution. This occurrence is not possible if the elasticity tensor (*i.e.* the second variation of the energy) is always positive definite.

In this section we determine the values of σ for which there could be a second solution in a neighborhood of the uniformly straight configuration ($\xi = 0$ and $\vartheta = 0$). For these critical values not only the elasticity tensor loses its positive definiteness but also the assumptions of the implicit function theorem fail. This analysis will open the stage to the bifurcation analysis carried on in the next section.

By the implicit function theorem, a necessary condition for $\sigma = \sigma_c$ to be a bifurcation point is

$$d^2 \mathcal{E}(\mathbf{o}, \sigma_c)[\mathbf{u}_c, \mathbf{v}] = 0 \quad \forall \mathbf{v}, \quad (40)$$

for some non trivial $\mathbf{u}_c = (\xi_c, \vartheta_c)$ satisfying the boundary conditions, where

$$d^2 \mathcal{E}(\mathbf{u}, \sigma)[\mathbf{v}, \mathbf{w}] = \frac{d}{dt} d\mathcal{E}(\mathbf{u} + t\mathbf{w}, \sigma)[\mathbf{v}] \Big|_{t=0} = \frac{d^2}{dsdt} \mathcal{E}(\mathbf{u} + s\mathbf{v} + t\mathbf{w}, \sigma) \Big|_{s,t=0}.$$

The second derivative of the energy can be written explicitly as

$$\begin{aligned} d^2 \mathcal{E}(\mathbf{u}, \sigma)[\hat{\mathbf{v}}, \bar{\mathbf{v}}] &= \int_0^1 \partial_{11}^2 w \hat{\xi} \bar{\xi} + \partial_{12}^2 w \left(\hat{\xi}' \bar{\xi} + \hat{\xi} \bar{\xi}' \right) + \partial_{13}^2 w \left(\hat{\xi} \bar{\vartheta}' + \hat{\vartheta}' \bar{\xi} \right) \\ &\quad + \partial_{22}^2 w \hat{\xi}' \bar{\xi}' + \partial_{23}^2 w \left(\hat{\xi}' \bar{\vartheta}' + \hat{\vartheta}' \bar{\xi}' \right) + \partial_{33}^2 w \hat{\vartheta}' \bar{\vartheta}' dx \end{aligned} \quad (41)$$

and evaluating all the second derivatives of w at $(\mu, \mu', \vartheta) = (\mu_0, 0, 0)$ we find

$$d^2 \mathcal{E}(\mathbf{o}, \sigma_c)[\hat{\mathbf{v}}, \bar{\mathbf{v}}] = \int_0^1 C_{11} \hat{\xi} \bar{\xi} + \sigma_c C_{13} \left(\hat{\xi} \bar{\vartheta}' + \hat{\vartheta}' \bar{\xi} \right) + C_{22} \hat{\xi}' \bar{\xi}' + C_{33} \hat{\vartheta}' \bar{\vartheta}' dx \quad (42)$$

where

$$\begin{aligned} C_{11} &= \partial_{11}^2 w(\mu_0, 0, 0) = 2 \left(\varepsilon + \frac{3\varepsilon + (\gamma - (4 - 3\alpha)\varepsilon)\mu_0}{\mu_0^4} \right), & C_{13} &= \frac{\partial_{13}^2 w(\mu_0, 0, 0)}{\sigma} = \frac{\varepsilon\gamma}{2}, \\ C_{22} &= \partial_{22}^2 w(\mu_0, 0, 0) = \frac{\varepsilon^2}{12} (\alpha\varepsilon + 3\gamma\mu_0), & C_{33} &= \partial_{33}^2 w(\mu_0, 0, 0) = \frac{\varepsilon^3 \mu_0^2}{6}. \end{aligned} \quad (43)$$

Then

$$\begin{aligned} d^2 \mathcal{E}(\mathbf{o}, \sigma_c)[\mathbf{u}_c, \mathbf{v}] &= \int_0^1 C_{11} \xi_c \xi + \sigma_c C_{13} (\xi_c \vartheta' + \vartheta'_c \xi) + C_{22} \xi^{c'} \xi' + C_{33} \vartheta'_c \vartheta' dx \\ &= \int_0^1 (C_{11} \xi_c + \sigma_c C_{13} \vartheta'_c - C_{22} \xi_c'') \xi - (\sigma_c C_{13} \xi^{c'} + C_{33} \vartheta_c'') \vartheta dx \end{aligned}$$

where we have taken into account that \mathbf{u}_c and $\mathbf{v} = (\xi, \vartheta)$ are null at $x = 0, 1$.

Condition (40) is therefore equivalent to the following system of differential equations:

$$\begin{cases} C_{11} \xi_c + \sigma_c C_{13} \vartheta'_c - C_{22} \xi_c'' = 0, \\ \sigma_c C_{13} \xi_c' + C_{33} \vartheta_c'' = 0. \end{cases} \quad (44)$$

For $\sigma_c \neq 0$, since $C_{13} \neq 0$, it is possible to get rid off ξ_c'' in (44)₁ by determining ξ_c' from (44)₂ and then solve for ξ_c :

$$\xi_c = -\frac{1}{C_{11}} \left(\sigma_c C_{13} \vartheta_c' + \frac{C_{22} C_{33}}{\sigma_c C_{13}} \vartheta_c''' \right), \quad (45)$$

where ϑ_c is the solution of the following problem:

$$\begin{cases} C_{22} C_{33} \vartheta_c'''' + (\sigma_c^2 C_{13}^2 - C_{11} C_{33}) \vartheta_c'' = 0 & \text{in } (0, 1), \\ \vartheta_c = 0 & \text{at } x = 0, 1, \\ \sigma_c C_{13} \vartheta_c' + \frac{C_{22} C_{33}}{\sigma_c C_{13}} \vartheta_c''' = 0 & \text{at } x = 0, 1. \end{cases}$$

For $\sigma_c C_{13}^2 - C_{11} C_{33} \leq 0$ the only solution is $\vartheta_c = 0$. For $\sigma_c C_{13}^2 - C_{11} C_{33} > 0$ set

$$\omega^2 = \frac{\sigma_c^2 C_{13}^2 - C_{11} C_{33}}{C_{22} C_{33}},$$

and write the general solution as

$$\vartheta_c(x) = a_1 \cos(\omega x) + a_2 \sin(\omega x) + a_3 x + a_4. \quad (46)$$

Imposing the boundary conditions we find the system

$$\begin{pmatrix} 1 & 0 & 0 & 1 \\ \cos \omega & \sin \omega & 1 & 1 \\ 0 & C_{11} C_{33} \omega & \sigma_c^2 C_{13}^2 & 0 \\ -C_{11} C_{33} \omega \sin \omega & C_{11} C_{33} \omega \cos \omega & \sigma_c^2 C_{13}^2 & 0 \end{pmatrix} \begin{pmatrix} a_1 \\ a_2 \\ a_3 \\ a_4 \end{pmatrix} = 0, \quad (47)$$

from which we deduce that we have a non trivial solution if and only if

$$2\sigma_c^2 C_{13}^2 (1 - \cos \omega) = C_{11} C_{33} \omega \sin \omega.$$

This equation is satisfied if

$$\omega = 2k\pi \quad \text{for } k = 1, 2, 3, \dots \quad (48)$$

while for $\omega \neq 2k\pi$ we may divide the equation by $\sin \omega$, after noticing that $\omega = (2k + 1)\pi$ is not a solution, to find

$$\tan \frac{\omega}{2} = \frac{C_{11}C_{33}}{2\sigma_c^2 C_{13}^2} \omega = \frac{(\omega/2)(C_{11}/C_{22})}{\omega^2 + C_{11}/C_{22}}, \quad (49)$$

where we used the equality $\tan(z/2) = (1 - \cos z)/\sin z$. It is easy to see that this equation has an infinite number of solutions. We denote the smallest solution different from zero by $\hat{\omega}$ and we remark that $\hat{\omega} > 2\pi$, as an analytical study of the functions involved show.

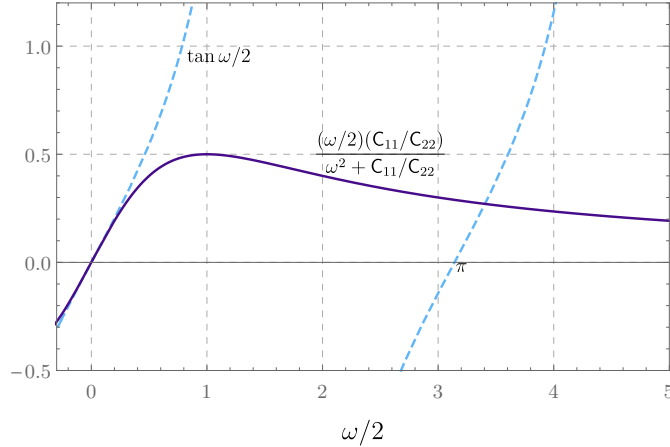


Figure 4: A graphical solution of equation (49). The left hand-side of (49) is depicted with a dashed line while the right hand-side with a solid line. The smallest point, larger than zero, in which the two graphs intersect is for $\omega/2 > \pi$.

The smallest value of ω for which we might have a non trivial solution, and

hence a bifurcation, is given by (48) for $k = 1$:

$$\omega_c = 2\pi.$$

From the definition of ω we deduce the smallest value of σ_c for which we might have a bifurcation

$$\omega_c^2 = 4\pi^2 = \frac{\sigma_c^2 C_{13}^2 - C_{11} C_{33}}{C_{22} C_{33}},$$

that is

$$\sigma_c = \pm \sqrt{\frac{4\pi^2 C_{22} + C_{11}}{C_{13}^2} C_{33}}. \quad (50)$$

On recalling definitions (43), we can express the critical value of the apico-basal imbalance parameter as

$$\sigma_c = \pm \frac{\sqrt{2}\gamma}{\sqrt{3\varepsilon\mu_0}} \sqrt{2\varepsilon \left(1 + \frac{3}{\mu_0^4} + \frac{\gamma - (4 - 3\alpha)\varepsilon}{\mu_0^3} \right) + 4\pi^2 \left(\frac{\alpha\varepsilon^3}{12} + \frac{1}{4}\gamma\varepsilon^2\mu_0 \right)}. \quad (51)$$

Since the parameters γ , ε , α and μ_0 are related by (36), we may express σ_c in terms of only three variables. We find, *e.g.*,

$$\sigma_c = \pm \frac{\sqrt{2}\mu_0^2}{\sqrt{3\varepsilon(2 - (4 - 3\alpha)(\mu_0 - \mu_0^3) - \mu_0^4)}} \times \sqrt{\frac{2\varepsilon}{\mu_0^4} (1 - (4 - 3\alpha - 3\mu_0)\mu_0^3) + \frac{\pi^2\varepsilon^3}{3} (6(\mu_0 - 1)^3(\mu_0 + 1) + \alpha(1 - 9(\mu_0 - \mu_0^3)))}. \quad (52)$$

It is also possible to express σ_c in terms of γ , ε , and α by solving (36) in terms of μ_0 . We refrain to write this expression of σ_c since it would involve cumbersome quartic roots of (36).

In Fig. 5 we plot σ_c , for fixed α and ε , as a function of γ and μ_0 ; in Table 1 we report the values of σ_c relative to $\varepsilon = 0.1$, for several values of α and γ . The possible values that σ can take are between 0 and 0.5, thus for $\sigma_c > 0.5$ no bifurcation occurs. The competition between bulk energy and surface energy is

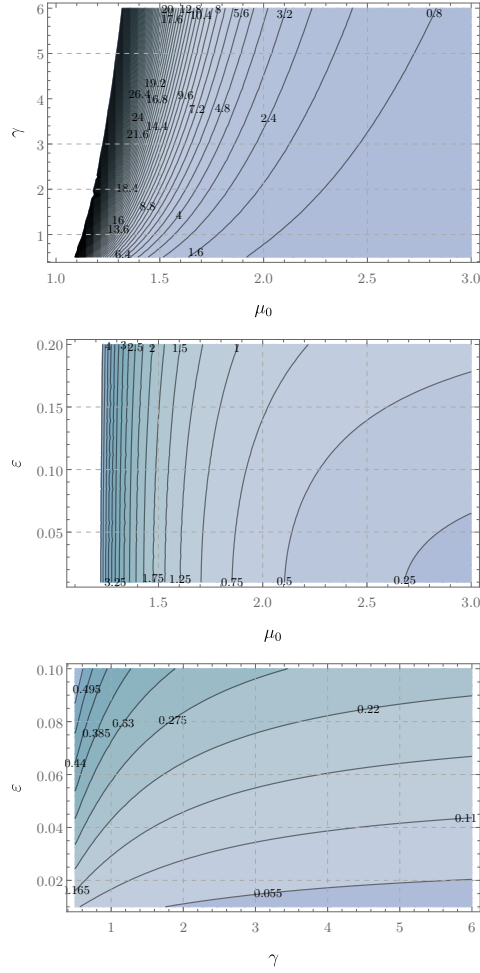


Figure 5: The contour plots for the critical apico-basal imbalance parameter σ_c , for $\alpha = 0.2$, and as a function of γ and μ_0 (top left), ϵ and μ_0 (top right), ϵ and γ (center below). The possible values that σ can take are between 0 and 0.5, thus in the regions in which σ_c is larger than 0.5 no bifurcation occurs.

captured by γ . In Table 1 we see that for γ small the stabilizing effect of the bulk energy prevails and the bifurcation is inhibited.

From the system (47), with $\omega = \omega_c$, we find $a_2 = a_3 = 0$ and $a_1 = -a_4$, and

		γ							
		0.3	0.5	1	2	3	4	5	6
α	0.0	0.8973	0.6743	0.4794	0.3649	0.3219	0.2988	0.2841	0.2738
	0.2	0.8478	0.6385	0.4542	0.346	0.3056	0.2842	0.2707	0.2613
	0.4	0.8299	0.618	0.4355	0.3301	0.2915	0.2713	0.2587	0.2500
	0.6	0.8365	0.6102	0.4225	0.3171	0.2793	0.2598	0.2479	0.2398
	0.8	0.8590	0.6121	0.4143	0.3066	0.2689	0.2498	0.2383	0.2306
	1.0	0.8905	0.6208	0.4100	0.2983	0.2601	0.2411	0.2297	0.2222

Table 1: Values of σ_c relative to $\varepsilon = 0.1$, for several values of α and γ . Gray cells correspond to non admissible values for σ_c .

from (46) and (45) we deduce, up to a constant,

$$\vartheta_c(x) = \kappa(1 - \cos(2\pi x)), \quad \xi_c = \sin(2\pi x),$$

where the constant κ is defined by

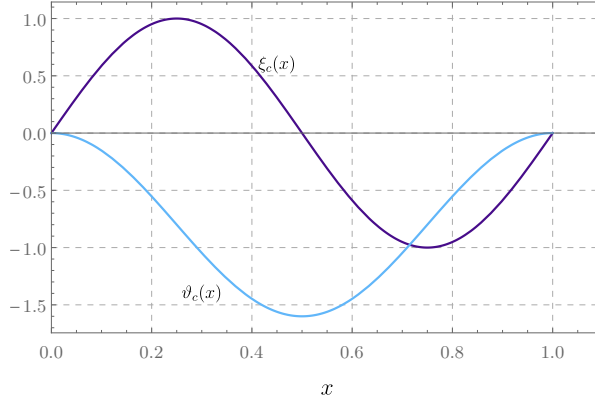
$$\kappa = -\frac{\sigma_c C_{13}}{2\pi C_{33}}. \quad (53)$$

Thus the eigenspace associated to σ_c , given by (50), is one dimensional:

$$\mathcal{N} = \text{span} \{\mathbf{u}_c\}, \quad \text{with } \mathbf{u}_c = (\xi_c, \vartheta_c) = (\sin(2\pi x), \kappa(1 - \cos(2\pi x))). \quad (54)$$

4 Bifurcation analysis

In the previous section we found the smallest value σ_c of the surface tension apico-basal imbalance for which a bifurcation may occur. In this section, by means of the *Lyapunov-Schmidt decomposition method*, we show that the critical value σ_c is indeed a bifurcation point, hence proving that besides the uniformly straight configuration there is a “folded” configuration. For σ less than the critical value σ_c , the stabilizing contribution of the epithelial elasticity keeps

Figure 6: The critical mode \mathbf{u}_c .

the equilibrium configuration straight, while for σ larger than σ_c the surface energy prevails and the epithelia bifurcates. In Section 4.1 we characterize the bifurcation and we make further remarks.

Within the framework of the Lyapunov-Schmidt decomposition, the increment $\mathbf{u} - \mathbf{u}_c$ associated to an increment of the parameter σ is decomposed in two components: one is in \mathcal{N} , and the other in the complement set

$$\mathcal{N}^\perp = \{\tilde{\mathbf{u}} = (\tilde{\xi}, \tilde{\vartheta}) : \int_0^1 \mathbf{u}_c \cdot \tilde{\mathbf{u}} \, dx = \int_0^1 \xi_c \tilde{\xi} + \vartheta_c \tilde{\vartheta} \, dx = 0\}.$$

A generic \mathbf{u} and σ can be written uniquely as

$$\begin{aligned} \mathbf{u} &= \eta \mathbf{u}_c + \tilde{\mathbf{u}} \quad \text{for some } \eta \in \mathbb{R} \text{ and } \tilde{\mathbf{u}} \in \mathcal{N}^\perp, \\ \sigma &= \sigma_c + \beta \quad \text{for some } \beta \in \mathbb{R}. \end{aligned} \tag{55}$$

We now decompose the test function \mathbf{v} appearing in (38) as in (55) and then we find

$$\begin{cases} d\mathcal{E}(\eta \mathbf{u}_c + \tilde{\mathbf{u}}, \sigma_c + \beta)[\mathbf{u}_c] = 0, \\ d\mathcal{E}(\eta \mathbf{u}_c + \tilde{\mathbf{u}}, \sigma_c + \beta)[\tilde{\mathbf{v}}] = 0 \quad \forall \tilde{\mathbf{v}} \in \mathcal{N}^\perp. \end{cases} \tag{56}$$

For fixed values of $\eta, \beta \in \mathbb{R}$ the second equation of (56) can be uniquely solved for the unknown $\tilde{\mathbf{u}}$. The solution

$$\tilde{\mathbf{u}} = \tilde{\mathbf{u}}(\eta, \beta) \quad (57)$$

satisfies

$$d\mathcal{E}(\eta \mathbf{u}_c + \tilde{\mathbf{u}}(\eta, \beta), \sigma_c + \beta)[\tilde{\mathbf{v}}] = 0 \quad \forall \tilde{\mathbf{v}} \in \mathcal{N}^\perp \text{ and } \forall \eta, \beta \in \mathbb{R} \quad (58)$$

and, in agreement with (39),

$$\tilde{\mathbf{u}}(0, \beta) = 0 \quad \forall \beta \in \mathbb{R}. \quad (59)$$

Let us now introduce the *reduced function*

$$f(\eta, \beta) = d\mathcal{E}(\eta \mathbf{u}_c + \tilde{\mathbf{u}}(\eta, \beta), \sigma_c + \beta)[\mathbf{u}_c]; \quad (60)$$

with this definition, solving (56)₁ reduces to searching the roots of the reduced function. By using (39) and (59), we first notice that

$$f(0, \beta) = d\mathcal{E}(0, \sigma_c + \beta)[\mathbf{u}_c] = 0 \quad \forall \beta; \quad (61)$$

hence $\eta = 0$ is a root for every β .

We now look for roots different from the trivial solution $\eta = 0$; more specifically, we plan to determine whether the equation $f(\eta, \beta) = 0$ has a branch of solutions crossing the trivial one at $(0, \beta)$.

We first notice that the reduced function f satisfies the following identities

$$f(0, 0) = \frac{\partial f}{\partial \beta}(0, 0) = \frac{\partial^2 f}{\partial \beta^2}(0, 0) = \frac{\partial f}{\partial \eta}(0, 0) = 0 \quad (62)$$

and

$$\frac{\partial^2 f}{\partial \eta \partial \beta}(0, 0) = d^2 \mathcal{E}_\sigma(0, \sigma_c)[\mathbf{u}_c, \mathbf{u}_c], \quad \text{with } \mathcal{E}_\sigma(\cdot, \sigma) = \frac{d}{d\sigma} \mathcal{E}(\cdot, \sigma).$$

as shown in A. From (26) we easily get

$$w_\sigma = \frac{\partial w}{\partial \sigma} = \gamma \left(\frac{1}{2} \varepsilon \mu \vartheta' - \frac{1}{16} \varepsilon^3 \mu^3 \vartheta' (\mu')^2 \right),$$

and then we deduce that

$$\partial_{13}^2 w_\sigma(\mu_0, 0, 0) = \frac{\gamma \varepsilon}{2} \quad \text{and} \quad \partial_{ij}^2 w_\sigma(\mu_0, 0, 0) = 0 \quad \text{for } (i, j) \notin \{(1, 3), (3, 1)\}.$$

Similarly to what we have already done in deducing (42), we find

$$\begin{aligned} d^2 \mathcal{E}_\sigma(\mathbf{o}, \sigma_c)[\mathbf{u}_c, \mathbf{u}_c] &= \int_0^1 2\partial_{13}^2 w_\sigma(\mu_0, 0, 0) \xi_c \vartheta'_c dx \\ &= 2\pi\gamma\varepsilon\kappa \int_0^1 \sin^2(2\pi x) dx = \pi\gamma\varepsilon\kappa. \end{aligned}$$

Hence

$$\frac{\partial^2 f}{\partial \eta \partial \beta}(0, 0) = d^2 \mathcal{E}_\sigma(0, \sigma_c)[\mathbf{u}_c, \mathbf{u}_c] = \pi\gamma\varepsilon\kappa \neq 0. \quad (63)$$

Through a clear use of the implicit function theorem, equation (63), together with (62), allows to conclude that there is a branch of solutions different from the trivial one through the point $(\eta, \beta) = (0, 0)$. More precisely, there exists a unique

$$\beta = \beta(\eta) \quad \text{with} \quad \beta(0) = 0,$$

such that

$$f(\eta, \beta(\eta)) = 0. \quad (64)$$

In particular, this implies that σ_c is a *bifurcation point*.

4.1 Apico-basal tension imbalance yields subcritical bifurcation

When a homogeneous material is subjected to an elastic compression exceeding a certain threshold, wrinkling may occur on the surface, a bifurcation that usually is *supercritical*. However, there are some circumstances in which bifurcations become *subcritical*, *e.g.*: (i) when the material is free-standing [39]; (ii) for a bilayer with the same elastic moduli for substrate and coating, but with a compressed substrate [40]; (iii) if there is a large enough surface energy [41].

Hereafter we show that, according to our model, the competition between epithelial tissue elasticity and surface tension produces a subcritical bifurcation, when the critical value σ_c of the apico-basal imbalance parameter is reached. This, in particular, implies that the uniformly straight configuration is stable for σ below σ_c and unstable immediately above, moreover also the bifurcated branches are unstable. In our model the bifurcated configuration does not develop oscillations, it has only one fold that may have a large amplitude. This is because the model is one-dimensional; in fact if the model would have been two-dimensional the boundary conditions would have constrained the surface displacement, forcing it to oscillate and fold [42]. Within this line of thought we may infer that the lack of stable branches for σ slightly larger than σ_c is a manifestation of the fact that not only creases form but also that the crease tip folds up and forms self-contact [43, 44, 45, 46].

To show that there is a branch that bifurcates from the straight configuration for $\sigma = \sigma_c$, we evaluate the derivatives of β at $\eta = 0$. We will show that the bifurcation is not *transcritical* (*i.e.* $\beta'(0) = 0$) but it is *subcritical* (*i.e.* $\beta''(0) < 0$). The computation of $\beta''(0)$ turns out to be quite involved since a linear operator needs to be inverted. In several standard problems this procedure is not necessary thanks to some symmetries enjoyed by the energy: symmetries

that in the case under study are lacking.

Differentiating (64) we find

$$\beta'(0) = -\frac{1}{2} \frac{\partial^2 f / \partial \eta^2}{\partial^2 f / \partial \eta \partial \beta}(0, 0). \quad (65)$$

The denominator has been computed in (63), while in A it is shown that

$$\frac{\partial^2 f}{\partial \eta^2}(0, 0) = d^3 \mathcal{E}(\mathbf{o}, \sigma_c)[\mathbf{u}_c, \mathbf{u}_c, \mathbf{u}_c]. \quad (66)$$

To evaluate the right hand side of (66), we note that the third derivatives of the density energy w evaluated at $(\mu_0, 0, 0)$ are zero, apart from the following:

$$\begin{aligned} \Gamma_1 = \partial_{111}^3 w(\mu_0, 0, 0) &= -\frac{6}{\mu_0^5} (\varepsilon(4 - (4 - 3\alpha)\mu_0) + \gamma\mu_0), & \Gamma_2 = \partial_{221}^3 w(\mu_0, 0, 0) &= \frac{\varepsilon^2 \gamma}{4}, \\ \Gamma_3 = \partial_{223}^3 w(\mu_0, 0, 0) &= -\frac{\sigma \gamma \varepsilon^3 \mu_0^3}{8}, & \Gamma_4 = \partial_{331}^3 w(\mu_0, 0, 0) &= \frac{\varepsilon^3 \mu_0}{3}. \end{aligned} \quad (67)$$

We can therefore write the right hand side of (66) as follows:

$$\begin{aligned} d^3 \mathcal{E}(\mathbf{o}, \sigma_c)[\mathbf{u}_c, \mathbf{u}_c, \mathbf{v}] &= \int_0^1 \Gamma_1 (\xi_c)^2 \xi + \Gamma_2 ((\xi'_c)^2 \xi + 2\xi_c \xi'_c \xi') \\ &\quad + \Gamma_3 ((\xi'_c)^2 \vartheta' + 2\xi'_c \vartheta'_c \xi') \\ &\quad + \Gamma_4 ((\vartheta'_c)^2 \xi + 2\xi_c \vartheta'_c \vartheta') \, dx, \end{aligned} \quad (68)$$

for $\mathbf{v} = (\xi, \vartheta)$. In particular, in the computation of $d^3 \mathcal{E}(\mathbf{o}, \sigma_c)[\mathbf{u}_c, \mathbf{u}_c, \mathbf{u}_c]$ we have to evaluate the integrals of the functions $(\xi_c)^3$, $(\xi'_c)^2 \xi_c$, $(\xi'_c)^2 \vartheta'_c$, and $(\vartheta'_c)^2 \xi_c$, which are all odd functions respect to $x = 1/2$, hence

$$\frac{\partial^2 f}{\partial \eta^2}(0, 0) = d^3 \mathcal{E}(\mathbf{o}, \sigma_c)[\mathbf{u}_c, \mathbf{u}_c, \mathbf{u}_c] = 0. \quad (69)$$

From (65) we deduce that $\beta'(0) = 0$, which means that the bifurcation is not

transcritical.

We now have to determine $\beta''(0)$. Differentiating three times (64), we deduce that the second derivative of β is

$$\beta''(0) = -\frac{1}{3} \frac{\partial^3 f / \partial \eta^3}{\partial^2 f / \partial \eta \partial \beta}(0, 0). \quad (70)$$

Again, the denominator has been computed in (63), while in A it is shown that

$$\frac{\partial^3 f}{\partial \eta^3}(0, 0) = d^4 \mathcal{E}(\mathbf{o}, \sigma_c)[\mathbf{u}_c, \mathbf{u}_c, \mathbf{u}_c, \mathbf{u}_c] + 3d^3 \mathcal{E}(\mathbf{o}, \sigma_c)[\mathbf{u}_c, \mathbf{u}_c, \mathbf{u}_c + \tilde{\mathbf{u}}_{\eta\eta}],$$

where

$$\tilde{\mathbf{u}}_{\eta\eta} = (\xi_{\eta\eta}, \vartheta_{\eta\eta}) = \frac{\partial^2 \tilde{\mathbf{u}}}{\partial \eta \partial \beta}(0, 0),$$

and $\tilde{\mathbf{u}}$ defined in (57). By taking into account (69), the above equation reduces to

$$\frac{\partial^3 f}{\partial \eta^3}(0, 0) = d^4 \mathcal{E}(\mathbf{o}, \sigma_c)[\mathbf{u}_c, \mathbf{u}_c, \mathbf{u}_c, \mathbf{u}_c] + 3d^3 \mathcal{E}(\mathbf{o}, \sigma_c)[\mathbf{u}_c, \mathbf{u}_c, \tilde{\mathbf{u}}_{\eta\eta}]. \quad (71)$$

To compute the fourth variation of the energy, we note that the fourth derivatives of the density energy w evaluated at $(\mu_0, 0, 0)$ are all zero, apart from:

$$\begin{aligned} \Lambda_1 &= \partial_{1111}^4 w(\mu_0, 0, 0) = \frac{24}{\mu_0^6} (\varepsilon(5 - (4 - 3\alpha)\mu_0) + \gamma\mu_0), & \Lambda_2 &= \partial_{1133}^4 w(\mu_0, 0, 0) = \frac{\varepsilon^3}{3}, \\ \Lambda_3 &= \partial_{2213}^4 w(\mu_0, 0, 0) = -\frac{3\gamma\varepsilon^3\mu_0^2}{8} \sigma_c. \end{aligned} \quad (72)$$

Taking into account (54) we find

$$\begin{aligned} d^4 \mathcal{E}(\mathbf{o}, \sigma_c)[\mathbf{u}_c, \mathbf{u}_c, \mathbf{u}_c, \mathbf{u}_c] &= \int_0^1 \Lambda_1(\xi_c)^4 + 6\Lambda_2(\xi_c)^2(\vartheta'_c)^2 + 12\Lambda_3\xi_c(\xi'_c)^2\vartheta'_c dx \\ &= \frac{3}{8}\Lambda_1 + 9\pi^2\kappa^2\Lambda_2 + 12\pi^3\kappa\Lambda_3. \end{aligned} \quad (73)$$

In order to evaluate the second term appearing in (71), we need to find $\tilde{\mathbf{u}}_{\eta\eta}$. To this end we differentiate (58) twice with respect to η to find

$$d^3\mathcal{E}(\mathbf{o}, \sigma_c)[\mathbf{u}_c, \mathbf{u}_c, \tilde{\mathbf{v}}] + d^2\mathcal{E}(\mathbf{o}, \sigma_c)[\tilde{\mathbf{u}}_{\eta\eta}, \tilde{\mathbf{v}}] = 0 \quad \forall \tilde{\mathbf{v}} \in \mathcal{N}^\perp. \quad (74)$$

Problem (74) admits a unique solution, since the bi-linear form $d^2\mathcal{E}(\mathbf{o}, \sigma_c)$ is positive definite on \mathcal{N}^\perp .

One of the major problems in evaluating (74) lies in the computation of $\tilde{\mathbf{u}}_{\eta\eta}$, because it is necessary to invert a linear operator. In a number of usual applications, this computation is not necessary, as $d\mathcal{E}(\mathbf{u}, \sigma)[\mathbf{v}]$ is an odd function, *i.e.*, $d\mathcal{E}(-\mathbf{u}, \sigma)[\mathbf{v}] = -d\mathcal{E}(\mathbf{u}, \sigma)[\mathbf{v}]$. If this was the case, we would have $d^3\mathcal{E}(\mathbf{o}, \sigma_c)[\mathbf{u}_c, \mathbf{u}_c, \tilde{\mathbf{u}}_{\eta\eta}] = 0$. The present problem does not fall within this circumstance. In B we carry out the cumbersome computation of $\tilde{\mathbf{u}}_{\eta\eta}$; in particular, we show that

$$\begin{aligned} \xi_{\eta\eta} &= \Upsilon_1 \cos(2\pi x) + \Upsilon_2 \cos(4\pi x) + \Upsilon_3, \\ \vartheta_{\eta\eta} &= \Psi_1 \sin(2\pi x) + \Psi_2 \sin(4\pi x), \end{aligned} \quad (75)$$

where the constants Υ_i and Ψ_i are defined in (98).

With this, we are in position to evaluate

$$d^3\mathcal{E}(\mathbf{o}, \sigma_c)[\mathbf{u}_c, \mathbf{u}_c, \tilde{\mathbf{u}}_{\eta\eta}] = -\frac{1}{4}\Gamma_1(\Upsilon_1 - 2\Upsilon_3) + \pi(\Gamma_3\Psi_2 + \pi\Gamma_2(\Upsilon_2 + 2\Upsilon_3)), \quad (76)$$

and finally, by using (63), (73), we can determine $\beta''(0)$ from (70):

$$\begin{aligned} \beta''(0) &= -\frac{1}{8\pi\gamma\varepsilon\kappa} \left(\Lambda_1 - 2\Gamma_1(\Upsilon_2 - 2\Upsilon_3) + 8\pi^2(-3\Gamma_2\Upsilon_2 + 4\pi\kappa(\Lambda_3 - 2\Gamma_3\Upsilon_2)) \right. \\ &\quad \left. + 2\Gamma_2\Upsilon_3 + \kappa^2(3\Lambda_2 - \Gamma_4\Upsilon_2 + 2\Gamma_4\Upsilon_3) + 4\pi\Gamma_3\Psi_2 - 4\Gamma_4\Psi_2 \right). \end{aligned} \quad (77)$$

In Fig. (7) we report the function $\beta''(0)$, for given α , in terms of γ and for different values of ε . Since $\beta''(0)$ is always negative, we conclude that *the*

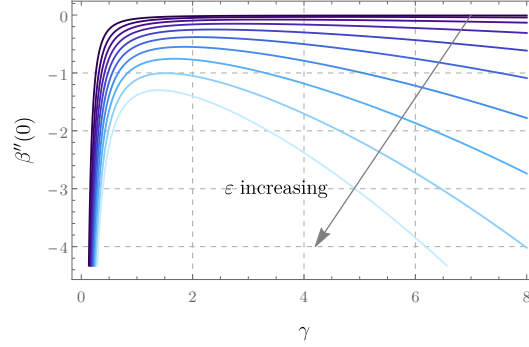


Figure 7: $\beta''(0)$, for given α , in terms of γ and for different values of ε

bifurcation is subcritical.

To gain further insight, we have computed the points of the solution branch using Keller's pseudo-arclength continuation [47] implemented in the software AUTO-07p [48]. In the numerical example, we fixed $\varepsilon = 0.1$ and, based on Table 1, we chose $\gamma = 5$, so that the critical value σ_c is approximately the intermediate value within the admissible range $[0, 1/2]$. We further set $\alpha = 0.2$.

We obtained the diagram shown in Fig. 8 where the symmetric bifurcated paths stop at two endpoints where AUTO failed to converge. For completeness we also report some equilibrium configurations for different values of σ (Fig. 9). Although such equilibria are not stable, and hence cannot be observed as stationary states, they may in principle represent snapshots along an evolution path, provided that the model is endowed with some dynamics.

5 Kras oncogene activation makes epithelial cells softer

In this section we show that our theory predicts a distinctive mechanical behavior of pre-cancerous cells.

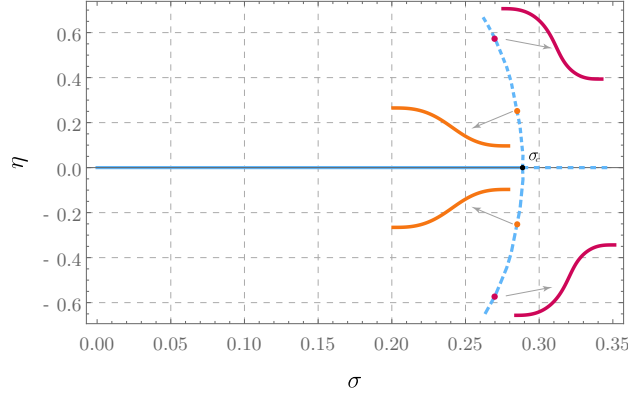


Figure 8: Symmetric branch emanating from the bifurcation point $(0, \sigma_c)$. The points marked on the upper side have coordinates $(0.21, 0.58)$ and $(0.20, 1.21)$. The corresponding deformed configurations are also shown.

Our analysis is based on the data available in [31], where a technique for 3D imaging, named fast light-microscopic analysis of antibody-stained whole organ (FLASH), is set to perform Immunofluorescence measures on dissected pancreatic tissues of mice where *Kras oncogene* activation is induced.

The authors measure phosphorylated myosin light chain (pMLC2) and find that after oncogene activation ductal structures have the same pMLC2 distribution in the apical and basal regions, which is consistent with the observed distribution of F-actin. In Fig. (10) we reported the data from [31], measured in approximately 70 healthy cells and 70 transformed cells from 7 mice.

The reported pMLC2 intensities values are:

$$I_a^h = 5.3, \quad I_a^t = 2.9, \quad I_b^h = 1,8, \quad I_b^t = 2.9,$$

where the superscripts h and t denote healthy (before transformation) and transformed cells, while the subscripts a and b indicate the apical and basal side, respectively. As in [31], we assume that apical and basal surface tensions are

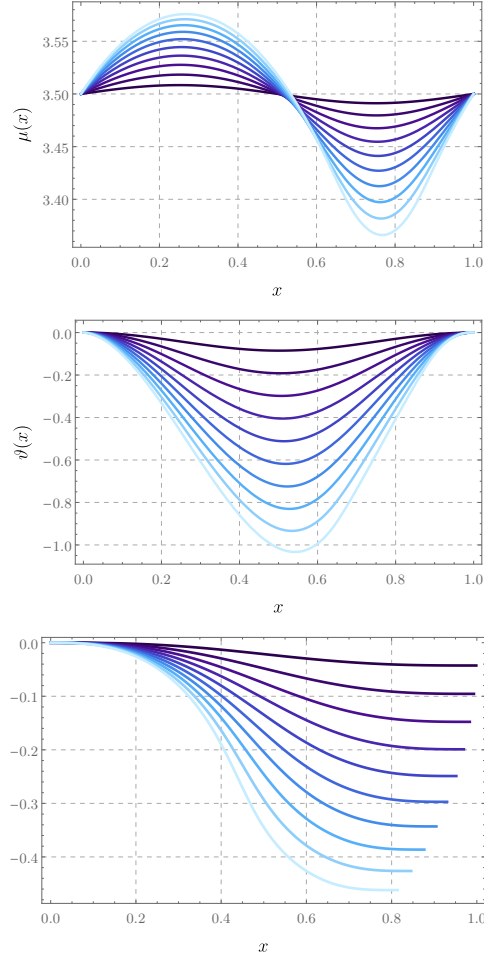


Figure 9: Numerical solutions of $\mu(x)$, $\vartheta(x)$ and shape of the midline for different values of σ .

proportional to pMLC2 intensities:

$$\sigma_a^h = 5.34\varpi, \quad \sigma_a^t = 2.96\varpi, \quad \sigma_b^h = 1.80\varpi, \quad \sigma_b^t = 2.96\varpi, \quad (78)$$

where ϖ is a proportionality constant. Recalling the definition of σ (21)₃, we find

$$\sigma^h = \frac{1}{2} \frac{\sigma_a^h - \sigma_b^h}{\sigma_a^h + \sigma_b^h} = 0.25, \quad \sigma^t = \frac{1}{2} \frac{\sigma_a^t - \sigma_b^t}{\sigma_a^t + \sigma_b^t} = 0. \quad (79)$$

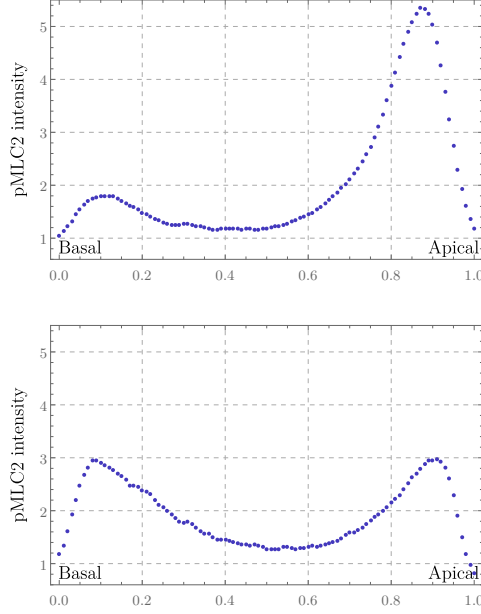


Figure 10: Concentration of Phospho-Myosin Light Chain 2 (pMLC2) in mice pancreatic epithelial tissue, healthy (left), transformed (right). Data from [31].

From Fig. 21 of [31] we deduce that the ratio between the thickness of transformed ducts, μ^t , and a healthy ducts, μ^h , is

$$\chi = \frac{\mu^t}{\mu^h} = 1.3.$$

Assuming, that the μ values differ only slightly from μ_0 (as we numerically observe) we deduce that

$$\frac{\mu_0^t}{\mu_0^h} = \chi. \quad (80)$$

For $\mu_0^3 \gg 1$, and hence $\mu_0^4 \gg \mu_0$, the quartic equation (36) simplifies to

$$\mu_0^4 - \frac{\gamma}{2\varepsilon}\mu_0 - \hat{\alpha}\mu_0^3 \simeq 0,$$

where

$$\hat{\alpha} = \frac{4 - 3\alpha}{2}$$

is always greater than 1/2 and smaller than 2. Simplifying μ_0 and adding the negligible term $3\mu_0(\hat{\alpha}/3)^2 - (\hat{\alpha}/3)^3$ to the previous identity we find

$$\mu_0^3 - \hat{\alpha}\mu_0^2 + 3\mu_0\left(\frac{\hat{\alpha}}{3}\right)^2 - \left(\frac{\hat{\alpha}}{3}\right)^3 \simeq \frac{\gamma}{2\varepsilon},$$

that is

$$\left(\mu_0 - \frac{\hat{\alpha}}{3}\right)^3 \simeq \frac{\gamma}{2\varepsilon}.$$

Thus

$$\mu_0 \simeq \frac{\hat{\alpha}}{3} + \left(\frac{\gamma}{2\varepsilon}\right)^{\frac{1}{3}}. \quad (81)$$

Equation (81), which has been tested for several values of α , γ , and ε , allows to write (80) as

$$\chi = \frac{\frac{\hat{\alpha}^t}{3} + \left(\frac{\gamma^t}{2\varepsilon}\right)^{\frac{1}{3}}}{\frac{\hat{\alpha}^h}{3} + \left(\frac{\gamma^h}{2\varepsilon}\right)^{\frac{1}{3}}} = \frac{\hat{\alpha}^t(2\varepsilon)^{\frac{1}{3}} + 3(\gamma^t)^{\frac{1}{3}}}{\hat{\alpha}^h(2\varepsilon)^{\frac{1}{3}} + 3(\gamma^h)^{\frac{1}{3}}} \simeq \frac{(\gamma^t)^{\frac{1}{3}}}{(\gamma^h)^{\frac{1}{3}}},$$

since ε is small and $1/2 \leq \hat{\alpha}^t, \hat{\alpha}^h \leq 2$. We therefore have found that

$$\chi^3 \simeq \frac{\gamma^t}{\gamma^h}.$$

From the definition of γ (21)₄ and the data in (78), we find

$$\frac{5.92\varpi}{\ell(\alpha_1^t + \alpha_2^t)} = \frac{\sigma_a^t + \sigma_b^t}{\ell(\alpha_1^t + \alpha_2^t)} \simeq \chi^3 \frac{\sigma_a^h + \sigma_b^h}{\ell(\alpha_1^h + \alpha_2^h)} = 1.3^3 \frac{7.14\varpi}{\ell(\alpha_1^h + \alpha_2^h)},$$

which leads to

$$\alpha_1^h + \alpha_2^h \simeq \frac{7.14}{5.92} \frac{1.3^3}{1} (\alpha_1^t + \alpha_2^t) = 2.62(\alpha_1^t + \alpha_2^t).$$

Thus, our theory predicts that in pancreatic epithelial ducts, shortly after onco-gene activation, the *transformed cells are softer than healthy ones*.

This finding agrees with [2], where it is shown that microscopic tissural modifications during pretumoral stage, owed only to abnormal apico-basal differential tension, cause a softening of the pancreatic tissue, possibly leading to a change in the physiological folded morphology.

A Properties of the reduced function $f(\eta, \beta)$

In order to evaluate the derivative of the reduced function $f(\eta, \beta)$ with respect to η , we note that, by (60),

$$\frac{\partial f}{\partial \eta}(\eta, \beta) = d^2 \mathcal{E}(\eta \mathbf{u}_c + \tilde{\mathbf{u}}(\eta, \beta), \sigma_c + \beta)[\mathbf{u}_c, \mathbf{u}_c + \frac{\partial \tilde{\mathbf{u}}}{\partial \eta}(\eta, \beta)],$$

hence, in particular,

$$\frac{\partial f}{\partial \eta}(0, 0) = d^2 \mathcal{E}(0, \sigma_c)[\mathbf{u}_c, \mathbf{u}_c + \frac{\partial \tilde{\mathbf{u}}}{\partial \eta}(0, 0)] = 0 \quad (82)$$

thanks to (40).

To continue, we need to note that

$$\frac{\partial \tilde{\mathbf{u}}}{\partial \beta}(0, \beta) = 0 \quad \text{and} \quad \frac{\partial \tilde{\mathbf{u}}}{\partial \eta}(0, 0) = 0. \quad (83)$$

The first follows directly from (59), while to show the second we differentiate (58) with respect to η to find

$$0 = \frac{\partial}{\partial \eta} d \mathcal{E}(\eta \mathbf{u}_c + \tilde{\mathbf{u}}(\eta, \beta), \sigma_c + \beta)[\tilde{\mathbf{v}}]|_{\eta=\beta=0} = d^2 \mathcal{E}(0, \sigma_c)[\tilde{\mathbf{v}}, \mathbf{u}_c + \frac{\partial \tilde{\mathbf{u}}}{\partial \eta}(0, 0)],$$

where we used (59). Using (40), the above equation reduces to

$$d^2 \mathcal{E}(\mathbf{o}, \sigma_c) \left[\tilde{\mathbf{v}}, \frac{\partial \tilde{\mathbf{u}}}{\partial \eta}(0, 0) \right] = 0,$$

which implies the second of (83), since $\partial \tilde{\mathbf{u}} / \partial \eta \in \mathcal{N}^\perp$.

Differentiating (82) with respect to β we find

$$\begin{aligned} \frac{\partial^2 f}{\partial \eta \partial \beta}(\eta, \beta) &= d^3 \mathcal{E}(\eta \mathbf{u}_c + \tilde{\mathbf{u}}(\eta, \beta), \sigma_c + \beta) [\mathbf{u}_c, \mathbf{u}_c + \frac{\partial \tilde{\mathbf{u}}}{\partial \eta}(\eta, \beta), \frac{\partial \tilde{\mathbf{u}}}{\partial \beta}(\eta, \beta)] \\ &\quad + d^2 \mathcal{E}(\eta \mathbf{u}_c + \tilde{\mathbf{u}}(\eta, \beta), \sigma_c + \beta) [\mathbf{u}_c, \mathbf{u}_c + \frac{\partial^2 \tilde{\mathbf{u}}}{\partial \eta \partial \beta}(\eta, \beta)] \\ &\quad + d^2 \mathcal{E}_\sigma(\eta \mathbf{u}_c + \tilde{\mathbf{u}}(\eta, \beta), \sigma_c + \beta) [\mathbf{u}_c, \mathbf{u}_c + \frac{\partial \tilde{\mathbf{u}}}{\partial \eta}(\eta, \beta)]. \end{aligned}$$

On taking into account (83), we find

$$\begin{aligned} \frac{\partial^2 f}{\partial \eta \partial \beta}(0, 0) &= d^3 \mathcal{E}(\mathbf{o}, \sigma_c) [\mathbf{u}_c, \mathbf{u}_c, 0] + d^2 \mathcal{E}(\mathbf{o}, \sigma_c) [\mathbf{u}_c, \mathbf{u}_c + \frac{\partial^2 \tilde{\mathbf{u}}}{\partial \eta \partial \beta}(0, 0)] \\ &\quad + d^2 \mathcal{E}_\sigma(\mathbf{o}, \sigma_c) [\mathbf{u}_c, \mathbf{u}_c]. \end{aligned}$$

Eq. (40) finally allows to conclude

$$\frac{\partial^2 f}{\partial \eta \partial \beta}(0, 0) = d^2 \mathcal{E}_\sigma(\mathbf{o}, \sigma_c) [\mathbf{u}_c, \mathbf{u}_c].$$

With similar calculations we find

$$\begin{aligned} \frac{\partial^2 f}{\partial \eta^2}(0, 0) &= d^3 \mathcal{E}(\mathbf{o}, \sigma_c) [\mathbf{u}_c, \mathbf{u}_c, \mathbf{u}_c] + d^2 \mathcal{E}(\mathbf{o}, \sigma_c) [\mathbf{u}_c, \mathbf{u}_c + \tilde{\mathbf{u}}_{\eta\eta}] \\ &= d^3 \mathcal{E}(\mathbf{o}, \sigma_c) [\mathbf{u}_c, \mathbf{u}_c, \mathbf{u}_c], \\ \frac{\partial^3 f}{\partial \eta^3}(0, 0) &= d^4 \mathcal{E}(\mathbf{o}, \sigma_c) [\mathbf{u}_c, \mathbf{u}_c, \mathbf{u}_c, \mathbf{u}_c] + 3d^3 \mathcal{E}(\mathbf{o}, \sigma_c) [\mathbf{u}_c, \mathbf{u}_c, \mathbf{u}_c + \tilde{\mathbf{u}}_{\eta\eta}] \\ &\quad + d^2 \mathcal{E}(\mathbf{o}, \sigma_c) [\mathbf{u}_c, \mathbf{u}_c + \frac{\partial^3 \tilde{\mathbf{u}}}{\partial \eta^3}(0, 0)] \\ &= d^4 \mathcal{E}(\mathbf{o}, \sigma_c) [\mathbf{u}_c, \mathbf{u}_c, \mathbf{u}_c, \mathbf{u}_c] + 3d^3 \mathcal{E}(\mathbf{o}, \sigma_c) [\mathbf{u}_c, \mathbf{u}_c, \mathbf{u}_c + \tilde{\mathbf{u}}_{\eta\eta}], \end{aligned}$$

where both equations have been simplified by using (40).

B Evaluation of $\tilde{\mathbf{u}}_{\eta\eta}$

For a generic function \mathbf{w} we define

$$\langle \mathbf{w} \rangle := \frac{1}{\int_0^1 \mathbf{u}_c \cdot \mathbf{u}_c dx} \int_0^1 \mathbf{u}_c \cdot \mathbf{w} dx,$$

and

$$\tilde{\mathbf{w}} := \mathbf{w} - \langle \mathbf{w} \rangle \mathbf{u}_c \in \mathcal{N}^\perp. \quad (84)$$

Clearly all functions in \mathcal{N}^\perp admit such a representation.

The problem that determines $\tilde{\mathbf{u}}_{\eta\eta}$ is (74):

$$d^3 \mathcal{E}(\mathbf{o}, \sigma_c)[\mathbf{u}_c, \mathbf{u}_c, \tilde{\mathbf{w}}] + d^2 \mathcal{E}(\mathbf{o}, \sigma_c)[\tilde{\mathbf{u}}_{\eta\eta}, \tilde{\mathbf{w}}] = 0 \quad \forall \tilde{\mathbf{w}} \in \mathcal{N}^\perp. \quad (85)$$

With $\tilde{\mathbf{w}}$ as in (84) we have

$$\begin{aligned} d^3 \mathcal{E}(\mathbf{o}, \sigma_c)[\mathbf{u}_c, \mathbf{u}_c, \tilde{\mathbf{w}}] &= d^3 \mathcal{E}(\mathbf{o}, \sigma_c)[\mathbf{u}_c, \mathbf{u}_c, \mathbf{w}] - \langle \mathbf{w} \rangle d^3 \mathcal{E}(\mathbf{o}, \sigma_c)[\mathbf{u}_c, \mathbf{u}_c, \mathbf{u}_c] \\ &= d^3 \mathcal{E}(\mathbf{o}, \sigma_c)[\mathbf{u}_c, \mathbf{u}_c, \mathbf{w}] \end{aligned}$$

by (69), and

$$\begin{aligned} d^2 \mathcal{E}(\mathbf{o}, \sigma_c)[\tilde{\mathbf{u}}_{\eta\eta}, \tilde{\mathbf{w}}] &= d^2 \mathcal{E}(\mathbf{o}, \sigma_c)[\tilde{\mathbf{u}}_{\eta\eta}, \mathbf{w}] - \langle \mathbf{w} \rangle d^2 \mathcal{E}(\mathbf{o}, \sigma_c)[\tilde{\mathbf{u}}_{\eta\eta}, \mathbf{u}_c] \\ &= d^2 \mathcal{E}(\mathbf{o}, \sigma_c)[\tilde{\mathbf{u}}_{\eta\eta}, \mathbf{w}] \end{aligned}$$

by (40). Thus, problem (85) leads to

$$d^3 \mathcal{E}(\mathbf{o}, \sigma_c)[\mathbf{u}_c, \mathbf{u}_c, \mathbf{w}] + d^2 \mathcal{E}(\mathbf{o}, \sigma_c)[\tilde{\mathbf{u}}_{\eta\eta}, \mathbf{w}] = 0 \quad \forall \mathbf{w}. \quad (86)$$

This latter problem, defined in the whole space and not just in \mathcal{N}^\perp , does not have a unique solution, in contrast with problem (85). Projecting on \mathcal{N}^\perp , with (84), any solution of (86) we find the unique solution of problem (85).

Integrating by parts (68) we find

$$\begin{aligned} d^3 \mathcal{E}(\mathbf{o}, \sigma_c)[\mathbf{u}_c, \mathbf{u}_c, \mathbf{v}] &= \int_0^1 [\Gamma_1(\xi_c)^2 + \Gamma_2(\xi'_c)^2 - 2\Gamma_2(\xi_c \xi'_c)' - 2\Gamma_3(\xi'_c \vartheta'_c)' \\ &\quad + \Gamma_4(\vartheta'_c)^2] \xi - [\Gamma_3((\xi'_c)^2)' + 2\Gamma_4(\xi_c \vartheta'_c)'] \vartheta \, dx. \end{aligned}$$

On taking into account (54), we conclude

$$d^3 \mathcal{E}(\mathbf{o}, \sigma_c)[\mathbf{u}_c, \mathbf{u}_c, \mathbf{v}] = \int_0^1 [\Xi_1 + \Xi_2 \sin^2(2\pi x)] \xi + \Xi_3 \sin(4\pi x) \vartheta \, dx,$$

where we have set

$$\begin{aligned} \Xi_1 &:= -4\pi^2(\Gamma_2 + 4\kappa\pi\Gamma_3), \quad \Xi_2 := \Gamma_1 + 12\pi^2\Gamma_2 + 32\kappa\pi^3\Gamma_3 + 4\kappa^2\pi^2\Gamma_4, \\ \Xi_3 &:= 8\pi^2(\pi\Gamma_3 - \kappa\Gamma_4). \end{aligned} \tag{87}$$

Similarly, from (42) we find

$$d^2 \mathcal{E}(\mathbf{o}, \sigma_c)[\tilde{\mathbf{u}}_{\eta\eta}, \tilde{\mathbf{v}}] = \int_0^1 [C_{11}\xi_{\eta\eta} + \sigma_c C_{13}\vartheta'_{\eta\eta} - C_{22}\xi''_{\eta\eta}] \xi - [\sigma_c C_{13}\xi'_{\eta\eta} + C_{33}\vartheta''_{\eta\eta}] \vartheta \, dx \tag{88}$$

and hence problem (86) writes also as

$$\begin{cases} C_{11}\xi_{\eta\eta} + \sigma_c C_{13}\vartheta'_{\eta\eta} - C_{22}\xi''_{\eta\eta} = -\Xi_1 - \Xi_2 \sin^2(2\pi x), \\ \sigma_c C_{13}\xi'_{\eta\eta} + C_{33}\vartheta''_{\eta\eta} = \Xi_3 \sin(4\pi x). \end{cases} \tag{89}$$

On solving (89)₂ for $\xi'_{\eta\eta}$ and inserting the result in (89)₁, we get $\xi_{\eta\eta}$ in terms

of $\vartheta_{\eta\eta}$:

$$\xi_{\eta\eta} = -\frac{1}{C_{11}} \left(\sigma_c C_{13} \vartheta'_{\eta\eta} + \frac{C_{22} C_{33}}{\sigma_c C_{13}} \vartheta'''_{\eta\eta} + \Xi_1 + \Xi_2 \sin^2(2\pi x) - 4 \frac{C_{22} \pi}{C_{13} \sigma_c} \Xi_3 \cos(4\pi x) \right). \quad (90)$$

On inserting (90) in (89)₂, we find the following problem for $\vartheta_{\eta\eta}$:

$$\begin{cases} \vartheta''''_{\eta\eta} + 4\pi^2 \vartheta''_{\eta\eta} = \frac{C_{11} \Xi_3 + 2\pi(8\pi C_{22} \Xi_3 + \sigma_c C_{13} \Xi_2)}{C_{22} C_{33}} \sin(4\pi x) & \text{in } (0, 1), \\ \vartheta_{\eta\eta} = 0 & \text{at } x = 0, 1, \\ \sigma_c C_{13} \vartheta'_{\eta\eta} + \frac{C_{22} C_{33}}{\sigma_c C_{13}} \vartheta'''_{\eta\eta} + \Xi_1 + \Xi_2 \sin^2(2\pi x) - 4 \frac{C_{22} \pi}{C_{13} \sigma_c} \Xi_3 \cos(4\pi x) = 0 & \text{at } x = 0, 1, \end{cases} \quad (91)$$

where we have made use of the relation

$$4\pi^2 = \frac{\sigma_c^2 C_{13}^2 - C_{11} C_{33}}{C_{22} C_{33}}.$$

A particular solution of (91) is

$$\vartheta_{\eta\eta}^p(x) = k \sin(4\pi x),$$

where

$$k := -\frac{C_{11} \Xi_3 + 2\pi(8\pi C_{22} \Xi_3 + \sigma_c C_{13} \Xi_2)}{192\pi^4 C_{22} C_{33}}.$$

The solution of the homogeneous equation is

$$\vartheta_{\eta\eta}^h(x) = b_1 \cos(2\pi x) + b_2 \sin(2\pi x) + b_3 x + b_4, \quad (92)$$

and then the general solution is

$$\vartheta_{\eta\eta}(x) = b_1 \cos(2\pi x) + b_2 \sin(2\pi x) + b_3 x + b_4 + k \sin(4\pi x), \quad (93)$$

where the constants b_1, \dots, b_4 have to be determined by enforcing the boundary conditions (91)_{2,3}.

From (90), we get

$$\xi_{\eta\eta}(x) = b_2\Phi_1 \cos(2\pi x) + \Phi_2 \cos(4\pi x) + b_1\Phi_3 \sin(2\pi x) + b_3\Phi_4 + \Phi_5, \quad (94)$$

where

$$\begin{aligned} \Phi_1 &= -\frac{1}{C_{11}} \left(2\pi\sigma_c C_{13} - \frac{8\pi^3 C_{22} C_{33}}{C_{13}\sigma_c} \right), \\ \Phi_2 &= \frac{-1}{48\pi^3 \sigma_c C_{11} C_{13} C_{22} C_{33}} \left(2\pi(8\pi C_{22} \Xi_3 + C_{13} \Xi_2 \sigma_c)(4\pi^2 C_{22} C_{33} - C_{13}^2 \sigma_c^2) + \right. \\ &\quad \left. C_{11} \Xi_3 (16\pi^2 C_{22} C_{33} - C_{13}^2 \sigma_c^2) \right), \\ \Phi_3 &= -\frac{2}{C_{11} C_{33} \sigma_c} \left(4\pi^3 C_{22} C_{33} - \pi C_{13}^2 \sigma_c^2 \right), \\ \Phi_4 &= -\frac{C_{13}}{C_{11}} \sigma_c, \\ \Phi_5 &= -\frac{1}{2C_{11}} (2\Xi_1 + \Xi_2). \end{aligned} \quad (95)$$

On using (93) and (94), the boundary conditions (91)_{2,3} read:

$$\begin{cases} b_1 + b_4 = 0 \\ b_1 + b_3 + b_4 = 0 \\ b_2\Phi_1 + b_3\Phi_4 = -\Phi_2 - \Phi_5, \end{cases} \quad (96)$$

since the two conditions (91)₃ coalesce. The system has ∞^1 solutions, parameterized by $b_4 = -b_1$. We need to project the solution on \mathcal{N}^\perp , *i.e.*, we have to request the orthogonality condition

$$0 = \int_0^1 \xi_{\eta\eta}(x)\xi_c(x) + \vartheta_{\eta\eta}(x)\vartheta_c(x) dx = \frac{1}{2}(\kappa(-b_1 + b_3 + 2b_4) + b_1\Phi_3), \quad (97)$$

which determines the unique solution of (96), and then allows to conclude that

$$\begin{aligned}\vartheta_{\eta\eta} &= \Psi_1 \sin(2\pi x) + \Psi_2 \sin(4\pi x), \\ \xi_{\eta\eta} &= \Upsilon_1 \cos(2\pi x) + \Upsilon_2 \cos(4\pi x) + \Upsilon_3,\end{aligned}\tag{98}$$

with

$$\begin{aligned}\Psi_1 &= \frac{1}{96\pi^4} \left(\frac{C_{11} + 16\pi^2 C_{22}}{C_{22} C_{33}} \Xi_3 + \frac{2\pi C_{13} \sigma_c}{C_{22} C_{33}} \Xi_2 + \frac{12\pi^2 (C_{11} \Xi_3 + 2C_{13} \pi \sigma_c (2\Xi_1 + \Xi_2))}{4\pi^2 C_{22} C_{33} - C_{13}^2 \sigma_c^2} \right), \\ \Psi_2 &= -\frac{1}{192\pi^4 C_{22} C_{33}} \left(C_{11} \Xi_3 + 2\pi (8\pi C_{22} \Xi_3 + C_{13} \Xi_2 \sigma_c) \right), \\ \Upsilon_1 &= \frac{1}{48\pi^3 \sigma_c C_{11} C_{13} C_{22} C_{33}} \left(16C_{22} C_{33} \pi^2 (C_{11} + 4C_{22} \pi^2) \Xi_3 + 16\pi^3 \sigma_c C_{13} C_{22} C_{33} (2\Xi_3 + 2\Xi_2) \right. \\ &\quad \left. - C_{13}^2 \sigma_c^2 (C_{11} + 16\pi^2 C_{22}) \Xi_3 - 2\pi \sigma_c^3 C_{13}^2 \Xi_2 \right), \\ \Upsilon_2 &= \frac{1}{48\pi^3 \sigma_c C_{11} C_{13} C_{22} C_{33}} \left(C_{11} \Xi_3 (C_{13}^2 \sigma_c^2 - 16\pi^2 C_{22} C_{33}), \right. \\ &\quad \left. - 2\pi (8\pi C_{22} \Xi_3 + \sigma_c C_{13} \Xi_2) (4\pi^2 C_{22} C_{33} - C_{13}^2 \sigma_c^2) \right), \\ \Upsilon_3 &= \frac{1}{2C_{11}} (2\Xi_1 + \Xi_2).\end{aligned}\tag{99}$$

We can then compute

$$d^3 \mathcal{E}(\mathbf{o}, \sigma_c)[\mathbf{u}_c, \mathbf{u}_c, \tilde{\mathbf{u}}_{\eta\eta}] = -\frac{1}{4} \Gamma_1 (\Upsilon_1 - 2\Upsilon_3) + \pi (\Gamma_3 \Psi_2 + \pi \Gamma_2 (\Upsilon_2 + 2\Upsilon_3)). \tag{100}$$

Eqs. (63), (70), (73), finally allow to determine $\beta''(0)$ as in (77).

References

- [1] R. Weinberg, *The Biology of Cancer*, W.W. Norton & Company, 20013.
- [2] N. Therville, S. Arcucci, A. Vertut, F. Ramos-Delgado, D. Da Mota, M. Dufresne, C. Basset, J. Guillermet-Guibert, *Experimental pancreatic*

- cancer develops in soft pancreas: novel leads for an individualized diagnosis by ultrafast elasticity imaging, *Theranostics* 9 (2019) 6369–6379.
- [3] W. H. Lewis, Mechanics of invagination, *The Anatomical Record* 97 (1947) 139–156.
- [4] H. Honda, G. Eguchi, How much does the cell boundary contract in a monolayered cell sheet?, *Journal of Theoretical Biology* 84 (3) (1980) 575–588.
- [5] T. Nagai, H. Honda, A dynamic cell model for the formation of epithelial tissues, *Philosophical Magazine B* 81 (7) (2001) 699–719.
- [6] A. Nestor-Bergmann, G. Goddard, S. Woolner, O. Jensen, Relating cell shape and mechanical stress in a spatially disordered epithelium using a vertex-based model, *Math Med Biol* 35 (Issue Supplement-1) (2018) 1–27.
- [7] E. Latorre, S. Kale, L. Casares, M. Gomez-Gonzalez, M. Uroz, L. Valon, R. V. Nair, E. Garreta, N. Montserrat, A. del Campo, B. Ladoux, M. Arroyo, X. Trepát, Active superelasticity in three-dimensional epithelia of controlled shape, *Nature* 563 (7730) (2018) 203–208.
- [8] M. Misra, B. Audoly, I. Kevrekidis, S. Shvartsman, Shape transformations of epithelial shells, *Biophysical Journal* 110 (7) (2016) 1670–1678.
- [9] M. Misra, B. Audoly, S. Y. Shvartsman, Complex structures from patterned cell sheets, *Phil. Trans. R. Soc. B* 372 (1720).
- [10] N. Murisic, V. Hakim, I. G. Kevrekidis, S. Y. Shvartsman, B. Audoly, From discrete to continuum models of three-dimensional deformations in epithelial sheets, *Biophysical Journal* 109 (1) (2015) 154–163.
- [11] C. Bielmeier, S. Alt, V. Weichselberger, M. L. Fortezza, H. Harz, F. J´ulicher, G. Salbreux, A.-K. Classen, Interface contractility between

- differently fated cells drives cell elimination and cyst formation, *Current Biology* 26 (5) (2016) 563–574.
- [12] P. Ciarletta, D. Ambrosi, G. A. Maugin, L. Preziosi, Mechano-transduction in tumour growth modelling, *The European Physical Journal E*, 36: 23 (2013).
- [13] A.R. Carotenuto, A. Cutolo, S. Palumbo, M. Fraldi, Lyapunov stability of competitive cells dynamics in tumor mechanobiology. *Acta Mechanica Sinica* 37, 244-263 (2021).
- [14] M. Fraldi, A. Cugno, L. Deseri, K. Dayal, N.M. Pugno, A frequency-based hypothesis for mechanically targeting and selectively attacking cancer cells. *J. R. Soc.Interface*12: 20150656 (2015).
- [15] D. Drasdo, Buckling instabilities of one-layered growing tissues, *Physical Review Letters* 84 (2000) 4244–4247.
- [16] B. I. Shraiman, Mechanical feedback as a possible regulator of tissue growth, *Proceedings of the National Academy of Sciences* 102 (9) (2005) 3318–3323.
- [17] E. Hohlfeld, L. Mahadevan, Unfolding the sulcus, *Physical Review Letters* 106 (2011) 105702.
- [18] B. Li, Y.-P. Cao, X.-Q. Feng, H. Gao, Mechanics of morphological instabilities and surface wrinkling in soft materials: a review, *Soft Matter* 8 (2012) 5728–5745.
- [19] M. Ben Amar, F. Jia, Anisotropic growth shapes intestinal tissues during embryogenesis, *Proceedings of the National Academy of Sciences* 110 (26) (2013) 10525–10530.

- [20] V. Balbi, E. Kuhl, P. Ciarletta, Morphoelastic control of gastro-intestinal organogenesis: Theoretical predictions and numerical insights, *Journal of the Mechanics and Physics of Solids* 78 (2015) 493–510.
- [21] G. Salbreux, F. Jülicher, Mechanics of active surfaces, *Physical Review E* 96 (2017) 032404.
- [22] V. Balbi, M. Destrade, A. Goriely, Mechanics of human brain organoids, *Phys. Rev. E* 101 (2020) 022403.
- [23] E. Hannezo, J. Prost, J. Joanny, Theory of epithelial sheet morphology in three dimensions, *Proceedings of the National Academy of Sciences U. S. A.* 111 (2017) 27–32.
- [24] M. Krajnc, N. Štorgel, A. Hočevar Brezavšek, P. Ziherl, A tension-based model of flat and corrugated simple epithelia, *Soft Matter* 9.
- [25] A. Papastavrou, P. Steinmann, E. Kuhl, On the mechanics of continua with boundary energies and growing surfaces, *Journal of the Mechanics and Physics of Solids* 61 (6) (2013) 1446–1463.
- [26] L. Sui, S. Alt, M. e. a. Weigert, Differential lateral and basal tension drive folding of drosophila wing discs through two distinct mechanisms, *Nature Communications* 9.
- [27] M. Krajnc, P. Ziherl, Theory of epithelial elasticity, *Physical Review E* 92 (2015) 052713.
- [28] N. Štorgel, M. Krajnc, P. Mrak, J. Štrus, P. Ziherl, Quantitative morphology of epithelial folds, *Biophysical Journal* 110 (2016) 269–77.
- [29] R. Farhadifar, J.-C. Röper, B. Aigouy, S. Eaton, F. Jülicher, The influence of cell mechanics, cell-cell interactions, and proliferation on epithelial packing, *Current Biology* 17 (24) (2007) 2095–2104.

- [30] V. Fiore, M. Krajnc, F. e. a. Quiroz, Mechanics of a multilayer epithelium instruct tumour architecture and function, *Nature* 585 (2020) 433–439.
- [31] H. A. Messal, S. Alt, R. e. a. Ferreira, Tissue curvature and apicobasal mechanical tension imbalance instruct cancer morphogenesis, *Nature* 566 (2019) 126–130.
- [32] P. A. Haas, R. E. Goldstein, Nonlinear and nonlocal elasticity in coarse-grained differential-tension models of epithelia, *Physical Review E* 99 (2019) 022411.
- [33] S. Antman, The theory of rods. in: Truesdell C. (eds) *linear theories of elasticity and thermoelasticity*.
- [34] S. Antman, *Nonlinear Problems of Elasticity*, Springer-Verlag, New York, 2005.
- [35] P. Podio-Guidugli, Flexural instabilities of elastic rods, *Journal of Elasticity* 12 (1) (1982) 3–17.
- [36] C.D. Coman, Bifurcation instabilities in finite bending of circular cylindrical shells, *International Journal of Engineering Science*, 119 (2017) 249–264.
- [37] S. Mora, C. Maurini, T. Phou, J.-M. Fromental, B. Audoly, Y. Pomeau, Solid drops: Large capillary deformations of immersed elastic rods, *Physical Review Letters* 111 (2013) 114301.
- [38] J. Bico, V. Reyssat, B. Roman, Elastocapillarity: When surface tension deforms elastic solids, *Annual Review of Fluid Mechanics* 50 (1) (2018) 629–659.
- [39] E. Hohlfeld, L. Mahadevan, Scale and nature of sulcification patterns, *Physical Review Letters* 109 (2012) 025701.

- [40] D. Chen, L. Jin, Z. Suo, R. C. Hayward, Controlled formation and disappearance of creases, *Materials Horizons* 1 (2014) 207–213.
- [41] D. Chen, S. Cai, Z. Suo, R. C. Hayward, Surface energy as a barrier to creasing of elastomer films: An elastic analogy to classical nucleation, *Physical Review Letters* 109 (2012) 038001.
- [42] T. Healey, Q. Li, R. Cheng, Wrinkling Behavior of Highly Stretched Rectangular Elastic Films via Parametric Global Bifurcation, *Journal of Nonlinear Science* 23 (2013) 777–805.
- [43] G. van der Heijden, S. Neukirch, V. Goss, J. Thompson, Instability and self-contact phenomena in the writhing of clamped rods, *International Journal of Mechanical Sciences* 45 (1) (2003) 161–196.
- [44] L. Jin, A. Auguste, R. C. Hayward, Z. Suo, Bifurcation Diagrams for the Formation of Wrinkles or Creases in Soft Bilayers, *Journal of Applied Mechanics* 82 (6).
- [45] P. Ciarletta, Matched asymptotic solution for crease nucleation in soft solids, *Nature Communications* 9 (496).
- [46] P. Ciarletta, L. Truskinovsky, Soft nucleation of an elastic crease, *Phys. Rev. Lett.* 122 (2019) 248001.
- [47] H. Keller, Numerical solution of bifurcation and nonlinear eigenvalue problems, In: Rabinowitz, P., Ed., *Applications of Bifurcation Theory*, Academic Press, New York 359–384.
- [48] E. J. Doedel, A. R. Champneys, F. Dercole, T. F. Fairgrieve, Y. A. Kuznetsov, B. Oldeman, R. Paffenroth, B. Sandstede, X. Wang, C. Zhang, *Auto-07p: Continuation and bifurcation software for ordinary differential equations*.